BULLETIN OF THE EARTHQUAKE
RESEARCH INSTITUTE
UNIVERSITY OF TOKYO
Vol. 61 (1986) pp. 1-65

Precursory Quiescence and Recovery of Aftershock Activities before Some Large Aftershocks

Ritsuko S. MATSU'URA
Earthquake Research Institute
(Received January 22, 1986)

Abstract

Temporal features of the aftershock activities following some large shallow earthquakes of $M \gtrsim 7$ in Japan have been studied quantitatively. The earthquakes concerned were accompanied by large aftershocks which triggered their own aftershock activities. The purpose of the present study is to seek any anomalous change in aftershock activities of the main shock before the occurrence of such large aftershocks. Aftershock activity shows an appreciable decrease from the level expected from the modified Omori formula before the occurrence of a large aftershock. The aftershock activity then recovers to the normal level or evev increases beyond the normal level shortly before the occurrence of the large aftershock. The recovered activity generally occurs near the hypocenter of the forthcoming large aftershock. Such a feature has been recognized in fourteen cases out of eighteen for which sufficient data are available. We have the possibility of predicting the occurrence of a large aftershock which might be as large and disastrous as the main shock, if we keep watch on the change of the aftershock activity immediately following the main shock. Moreover, a rough prediction of the place can be made by checking the hypocenter location of aftershocks occuring in the recovered stage.

1. Introduction

Seismicity pattern is one of the most promising subjects in earthquake prediction studies, because it brings us information about physical conditions such as the state of stress, the stage of corrosion, or the degree of strain concentration in and around the source region of an impending large earthquake. The emergence of seismic quiescence in a source region a few years preceding a large earthquake has often been reported (e. g. INOUYE, 1965; UTSU, 1968; MOGI, 1968b, 1969; OHTAKE, 1980). This is one of the best examples of seismicity precursors to a disastrous earthquake. Foreshock activity is another remarkable precursor.

However, it is often quite difficult to identify those seismicity

changes as precursors before the earthquake occurs. Many precursory changes of seismicity were found after the occurrence of a large earthquake. Pointing out precursory anomalies after the occurrence of a shock is called 'post prediction'. Post prediction is far easier than true prediction, since the area and the term within which we search for abnormal changes have already been revealed. Successful detection of a seismic gap was made for a major event which occurred in the last patch of an active seismic belt along which several major shocks had occurred successively in recent years (UTSU, 1970; OHTAKE *et al.*, 1977). In these cases, the area of the gap drew great attention beforehand.

Foreshocks are often indistinguishable from clusters of shocks which would not lead to large shocks. A method to distinguish foreshocks from swarm activities using waveform similarity has been presented by TSUJIURA (1979). However, contradictory results have also been reported in some other regions (ISHIDA and KANAMORI, 1978; MOTOYA and ABE, 1985). Other determinants such as the b-value are not always powerful.

We cannot recognize precursory seismicity changes before a large earthquake due to the lack of knowledge about temporal characteristics of earthquake occurrences under normal conditions. If the degree of fluctuation of seismicity in normal periods is well-known, any marked precursory change in seismicity which reflects physical processes of preparation for a large earthquake must be detected. However, seismicity shows such a wide variation that it is very difficult to represent its temporal features quantitatively, except for the case of aftershock activities.

Aftershock activities have been studied intensively, and it is widely accepted that the occurrence rate of aftershocks $n(t)$ obeys the modified Omori formula (UTSU, 1961),

$$n(t)=\frac{K}{(t+c)^p} \qquad (1)$$

where t is the lapse time from the main shock. Aftershocks are usually much smaller than the main shock and not followed by secondary aftershocks. However, sometimes a large aftershock occurs in an area adjacent to the rupture zone of the main shock. Such a large aftershock is followed by its own aftershocks (secondary aftershock). Hereafter, "large aftershock" means this type of remarkable aftershock.

Since the temporal characteristics of normal aftershock sequences can be represented quantitatively by the modified Omori formula, it is very interesting to examine whether there is any anomalous change in aftershock activity before the occurrence of a large aftershock. If any change is recognized and its common features are known, it is not only useful

for prediction of such a large aftershock which might cause additional disaster, but also important to reveal the generating process of such a large aftershock or an earthquake in general. In this paper, a quantitative study is made on many aftershock sequences having large aftershocks in and around Japan.

2. Method

Conventionally, three parameters, K, c, and p in (1) were determined from a log $n(t)$ vs. log t plot as Figures 6–15 in UTSU (1969). Since $n(t)$ is not a directly observed quantity, it is calculated from the number of aftershocks in a certain unit of time. Therefore, several aftershocks are represented by only one datum point, and the three parameters are obtained only after hundreds of aftershocks have occurred.

Recently, the maximum likelihood method to estimate those parameters has been introduced (OGATA, 1983). According to this method, the likelihood is defined as

$$L(K, c, p;\ t_1, t_2, \cdots t_N) = \prod_{i=1}^{N} n(t_i) \exp\left\{-\int_S^T n(s)ds\right\} \qquad (2)$$

when the i-th aftershock occurred at time t_i, all N aftershocks were observed from time S to T, and $n(t)$ is the same as (1). The logarithmic form of this likelihood can be written as follows.

$$\ln L(K, c, p; t) = \sum_{i=1}^{N} \ln\{n(t_i)\} - \int_S^T n(s)ds \qquad (3)$$

The most likely values of K, c, and p are those which maximize (2) or (3). Three parameters in (1) can be estimated directly from origin times of aftershocks; thus quantitative treatment of an aftershock activity for a short term becomes available.

In order to check the fit between the modified Omori formula and the temporal pattern of aftershock occurrence, the cumulative number of aftershocks plotted against the frequency-linearized time τ (OGATA and SHIMAZAKI, 1984) is useful. The frequency-linearized time (FLT) is defined as

$$\tau = \int_0^t n(s)ds \qquad (4)$$

which is equal to the calculated cumulative number of aftershocks using the estimated parameters in (1). The time interval between two successive aftershocks is equal to the unit time of τ. Therefore, if an aftershock sequence is perfectly expressed by (1) with appropriate parameters,

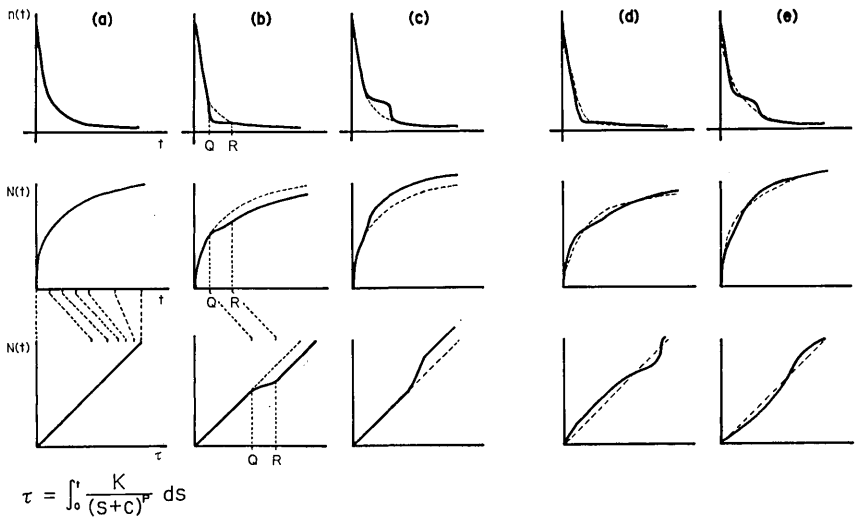

Fig. 1. Schematic graph showing variations of aftershock activity with time. The top row shows the rate of aftershock occurrence vs. lapse time from the mainshock. The middle and bottom rows are corresponding cumulative numbers for an ordinary time scale and a frequency-linearized time (FLT) scale, respectively. Dashed lines show the occurrence rate or the cumulative number calculated from the modified Omori formula (MOF) with estimated parameters.

(a) The activity without change.

(b) The same activity as (a) with a temporary decrease.

(c) The same activity as (a) with a temporary increase.

For (a), (b), and (c), the same set of parameters, which explains the activity (a) perfectly, is used for MOF and FLT.

(d) The same activity as (b) is shown with the different MOF and FLT estimated from the whole data including the decrease.

(e) The same activity as (c) is shown with the different MOF and FLT estimated from the whole data including the increase.

the cumulative number of aftershocks increases linearly with τ (Fig. 1 (a)). When there is a decrease or increase in activity below or above the level expected from the modified Omori formula whose parameters are evaluated from the data obtained until the emergence of the decrease or increase, the gradient of a cumulative number vs. τ curve shows a corresponding decrease or increase (Fig. 1(b), (c)). If τ is calculated from parameters using the data including the stage of decrease or increase, a cumulative number vs. τ line meanders around the straight line representing the modified Omori formula fitted to the data for the whole period of investigation (Fig. 1 (d), (e)).

Once the likelihood is obtained, Akaike's Information Criterion (AIC) (AKAIKE, 1974) defined by

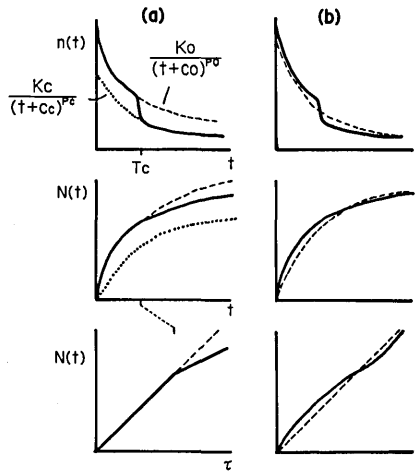

Fig. 2. Graph similar to Figure 1 showing the activity represented by (6-1).
(a) The (6-1)-type model is fitted to data. FLT of the bottom graph is estimated from data until T_C.
(b) The (1)-type model is fitted to data.

$$\text{AIC} = -2 \cdot \max.\,(\ln \text{ likelihood}) + 2 \cdot (\text{number of parameters}) \qquad (5)$$

is useful for selecting the most appropriate model. For a given set of data, a model with smaller AIC is better. If there is a significant change in the activity during an aftershock sequence with the occurrence of a large aftershock, AIC must be smaller for a model using two or more formulae such as (6-1) (Fig. 2 (a)) than for the model using a single formula for the whole sequence (Fig. 2 (b)).

$$n(t) = \begin{cases} \dfrac{K_0}{(t+c_0)^{p_0}} & \text{for } t \leq T_C \\ \dfrac{K_C}{(t+c_C)^{p_C}} & \text{for } t > T_C \end{cases} \qquad (6\text{-}1)$$

T_C; the time the activity changes

By the use of AIC, we can distinguish a significant change in activity on a plot of the cumulative number of aftershocks against the frequency-linearized time from a mere noise or a fluctuation of activity not related to the occurrence of a large aftershock.

When there are a significant decrease (at Q) and its recovery (at R) in the activity as shown in Figure 1(b), AIC must be smaller for models which take into account two changes such as (6-2) than for the (1)-type model or the (6-1)-type model.

$$n(t)=\begin{cases}\dfrac{K_0}{(t+c_0)^{p_0}} & \text{for } t\leq Q\\ \dfrac{K_Q}{(t+c_Q)^{p_Q}} & \text{for } Q<t\leq R\\ \dfrac{K_R}{(t+c_R)^{p_R}} & \text{for } R<t\end{cases} \tag{6-2}$$

When the activity after R (recovered activity) is equal to the level expected from the activity before Q, AIC is smaller for the model of (6-3) instead of (6-2).

$$n(t)=\begin{cases}\dfrac{K_0}{(t+c_0)^{p_0}} & \text{for } t\leq Q \text{ or } R<t\\ \dfrac{K_Q}{(t+c_Q)^{p_Q}} & \text{for } Q<t\leq R\end{cases} \tag{6-3}$$

For the analysis of actual data in this study, the smallest AIC is searched for among models of the (1), (6-1), (6-2), and (6-3) types.

When one aftershock sequence contains some large aftershocks accompanied by their secondary aftershocks, the modified Omori formula becomes

$$n(t)=\sum_{i=0}^{M} H(t-T_i)\cdot\frac{K_i}{(t-T_i+c_i)^{p_i}} \tag{7}$$

where $H(t)$ is a unit step function, M is the number of large aftershocks having their own aftershocks, and T_0 $(=0)$ and T_i are the origin time of the main shock and the i-th large aftershock, respectively. Even if $n(t)$ is replaced by (7), the likelihood and the frequency-linearized time can be defined by (2) and (4), respectively. The three parameters of (2), K, c, and p become (M+1)-dimension vectors. The actual number of parameters becomes 4M+3 (3(M+1) for K, c, and p, and M for T_i).

3. Data

Although many articles have been published describing aftershock sequences of large earthquakes, very few aftershock sequences can be re-examined by the method described in the previous chapter. Most papers reported only the occurrence rate of aftershocks with no list of the origin time of each aftershock. Furthermore, the lack of data right after the main shock often led seismologists into ignoring c in (1). In other words, the occurrence rate of aftershocks was represented by an equation proportional to t^{-p} (e.g. MOGI, 1962; PAGE, 1968). The c-value

cannot be obtained correctly from a $\log n(t)$ vs. $\log t$ plot without a few data points within one day of the main shock.

Since the purpose of this study is to find any significant change in aftershock activity before the occurrence of large aftershocks, homogeneity of data is essential. For a few hours right after a large earthquake, a ready-made catalog of aftershocks tends to be inhomogeneous, since it is often difficult to determine hypocenters during that time due to the extremely high rate of aftershock occurrence. Based on such a list, we might find false quiescence, or miss quiescence which appears after the occurrence rate has relatively abated. An inaccurate estimation of the c-value might also make it difficult to find small changes in the activity for small t.

Not only the temporal homogeneity of a list, but also the spatial extent covered by a list is important. The modified Omori formula represents the temporal feature of aftershock occurrence in the whole source region of the main shock. Aftershocks in a portion of the source region show clustering features different from the formula in some cases (PAGE, 1968). For a list of aftershocks sampled from a part of the source region, the study of deviations from the modified Omori formula makes no sense. On the contrary, if the area of sampling is too much larger than the actual aftershock area, the occurrence rate is not well-represented by the modified Omori formula, since the area includes aftershocks of other main shocks or other types of activities not directly related to the main shock.

The data to be analyzed in this study should contain the following conditions: the origin time and size of each aftershock must be known, aftershocks must be sampled thoroughly from the whole source region of the main shock, and aftershocks of magnitude above a certain fixed level must be counted without omission throughout the period of analysis. To satisfy these conditions, a homogeneous list of aftershocks made from strip-chart type records is ideal. Furthermore, multi-channel records of stations surrounding the source region are useful to distinguish earthquakes outside the source region from those within without calculations of hypocenter locations. When the magnitude of each aftershock is determined from total duration time (F-P) (TSUMURA, 1967) instead of maximum amplitudes, the size definition of aftershocks becomes more stable against the variations in mechanism among aftershocks or the confusion of records for a few hours after a large earthquake. This holds true because total duration time represents the information about the size of an earthquake in a whole waveform, while the maximum amplitude contains such information for an instant.

In this study, homogeneous lists of aftershocks for two sequences

are made with great care from strip-chart multi-channel records of the network of the Dodaira Microearthquake Observatory, which has been operated continuously with paper speed 60 mm/min since 1968. For other cases, data from bulletins of the Japan Meteorological Agency (JMA) or other catalogs are used with due consideration of their limitations. Magnitudes of main shocks and large aftershocks are taken from surface wave magnitudes (M_S) listed in ABE (1981). For smaller events not listed therein, magnitudes determined by JMA (M_J) are used. M_J is about 0.2 unit smaller than M_S in the magnitude range from $6^1/_2$ to $8^1/_4$ (UTSU, 1982c). M_U in the text indicates the magnitude for old earthquakes determined by UTSU (1979, 1982a, 1982b). Magnitudes of aftershoks used in the analysis of each sequence will be described individually. All dates and times in this paper are Japanese Standard Time, which is nine hours ahead of G.M.T.

4. Results obtained from homogeneous data sets

i) The east off Hachijo Island earthquake of 1972

On February 29, 1972, the east off Hachijo Island earthquake (hereafter, it is called the first shock) of M_S 7.4 (M_J 7.1) occurred and many aftershocks followed it. After nine months, when the aftershock activity was still observed, the off Hachijo Island earthquake (the second shock) of M_S 7.5 (M_J 7.2) occurred on December 4, 1972, abutting on the source region of the first shock.

This is one of the best examples for studying changes in aftershock activity with a large aftershock. Since the second shock was large enough, there is a high possibility that preparatory processes for the second shock which started after the occurrence of the first shock changed physical conditions in the whole or a large part of the aftershock area of the first shock. Since there were nine months between the two earthquakes, many aftershocks had occurred before the second shock. This makes the statistical treatment of aftershock activity easier.

However, there is no list of earthquakes in this area suitable for the present study. The area off Hachijo Island is remote from the microearthquake observation network and it is difficult to locate hypocenters in this area accurately. This area was excluded from the routine reports of seismicity in the Kanto district by the Earthquake Research Institute in the 1970's. The two nearest seismographs are on Hachijo and Miyake Islands. However, these are low-sensitivity ones operated by JMA and reports of P and S arrival times were few and not precise. In the Seismological Bulletin of JMA, only hypocenters of earthquakes of M 5 or above were reported for this area at that time.

In this study, the homogeneous list of earthquakes in this area from June 1971 to June 1976 has been made carefully. All pages of strip-chart type multi-channel records of the Dodaira Microearthquake Observatory network were examined and earthquakes of M 2.8 or larger in this area were listed. The magnitude of each earthquake was determined from total duration time according to the formula for the Dodaira Observatory (HORI, 1973). Since waveforms of earthquakes in this area observed at stations of the Dodaira Observatory are distinct from other local earthquakes in the Kanto district due to low-frequency dominance and an unclear S phase, finding earthquakes in this area from original records is not affected by a temporary breakdown of a station in the network. All earthquakes of $M \geq 3.0$ have been listed except for periods when two or more stations were concurrently out of order. The total length of such interruptions was one week in five years. When the magnitude is equal to or greater than 3.5, we can reliably discriminate shocks within the aftershock areas of the first and second shocks, even during the several minutes right after a large earthquake or when a few stations are in trouble, from ones in the surrounding areas: the swarm area off the west of Hachijo Island which was active in August 1974, or the aftershock area of the off Boso Peninsula earthquake of 1953 (M_S 7.9), which was the largest event near the area.

From this homogeneous list, it is found that before the second shock, the aftershock activity of the first shock decreased from the rate expected from the modified Omori formula. Then it recovered before the second shock. The degree of this decrease or quiescence is twice as large as the fluctuation of aftershock activity in other periods. If a single modified Omori formula is applied to represent the whole aftershock sequence of the first shock until the second shock, the deviation of the cumulative number curve from the straight line representing the modified Omori formula during the quiescent period is twice as large as that of other periods (Fig. 3(a)). Therefore, the model including the change represented by (6-1) is fitted to the data. The smallest AIC value is obtained when $T_c = 165$ days and the aftershock sequence is represented as follows (Fig. 3(b)).

$$n(t) = \begin{cases} \dfrac{16.9}{(t+0.05)^{0.79}} & \text{for } 0 = T_0 < t \leq T_c \quad (8\text{-}1) \\ 0.1 & \text{for } T_c < t \leq T_1 \quad (8\text{-}2) \end{cases}$$

After the time T_c, which is indicated by Q hereafter, the best fitted representation of the aftershock occurrence rate is independent of lapse time; in other words, $p_c = 0$. When the sequence after Q is plotted on

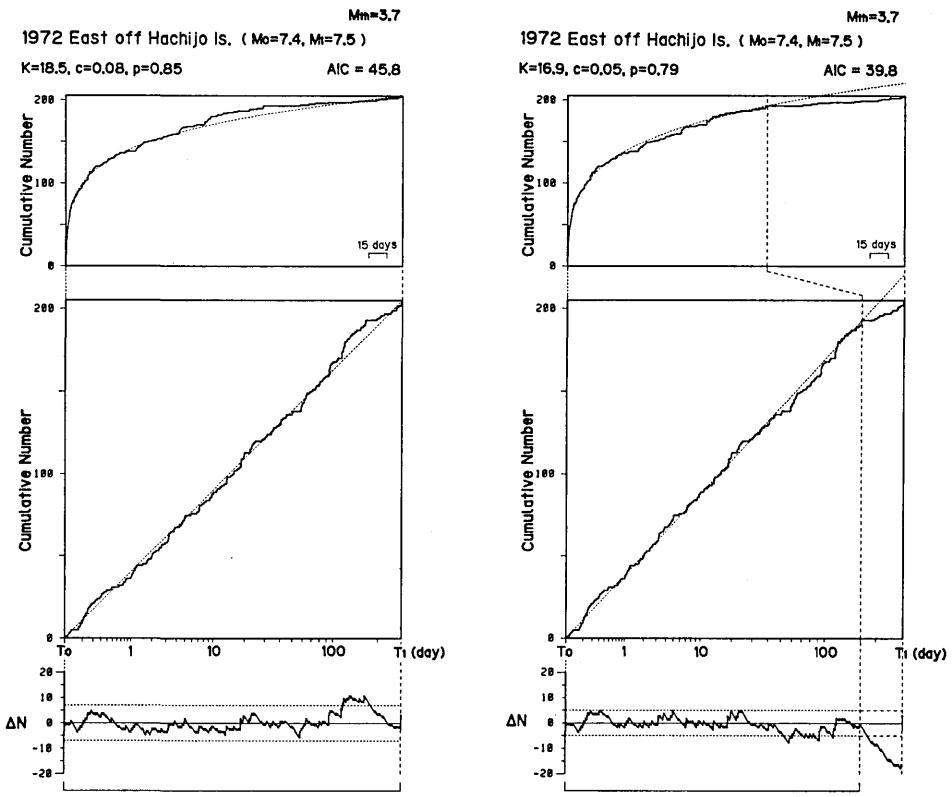

(a) (b)

Fig. 3. Top and middle figures show the cumulative number of aftershocks against ordinary time and FLT, respectively. The calculated cumulative number represented by dashed lines is calculated using the parameters shown above which are obtained by the maximum likelihood method from data in the range designated by a square bracket at the bottom. Figures on the FLT axis show lapse time in days from the left end. The bottom figure magnifies the difference of the observed cumulative number from the calculated one on the same time scale as the middle. The difference is rounded off to an integer. Double the standard deviation of the difference in the designated range is also shown by dotted lines. The threshold of magnitude (M_{th}) for counted aftershocks, the magnitude of the first and the second shocks (M_0 and M_1), and AIC value are shown at the top.

(a) The frequency-linearized time from all data.

(b) FLT from data until $t=165$ days.

the frequency-linearized time defined by the data before the change, it is found the decreased rate shows recovery before the second shock (Fig. 3(b)). Thus the sequence after Q is divided at R into two parts: the quiescent stage and the recovered stage. AIC is smaller for the (6-2)-type model than the (6-3)-type, and

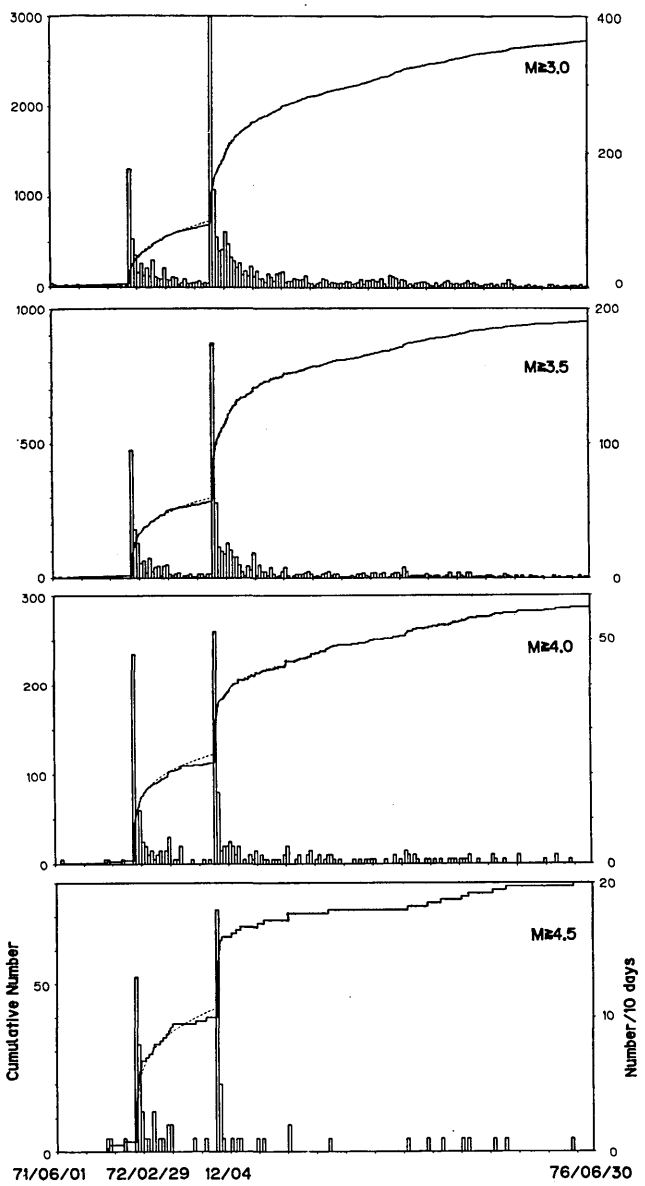

Fig. 4. Cumulative number of earthquakes in the area east off Hachijo Island against the ordinary time scale from June 1, 1971 to June 30, 1976. The lower limit of magnitude for counting earthquakes is shown in each graph. The dotted line between the first and the second shocks in each figure represents the calculated cumulative number for parameters estimated from data within 165 days from the first shock.

$$n(t)=\begin{cases} 0.06 & Q<t\leq R \\ 0.2 & R<t\leq T_1 \end{cases} \qquad (9)$$

where $R=235$ days. AIC for (8-1) plus (9) is slightly larger than that of (8-1) plus (8-2) by 0.14, a negligible amount of difference. The occurrence rate in the quiescent stage from Q to R is one-fifth to one-fourth of the rate estimated from (8-1). The rate in the recovered stage almost equals the estimated rate.

The emergence of quiescence and recovery in the aftershock activity before the second shock is recognized in several cases of different magnitude threshold (Fig. 4). When the threshold is large, the number of aftershocks to be analyzed becomes too small, and it is difficult to distinguish the quiescence from a mere fluctuation of activity. When the threshold is between M 3.5 and M 4.0, the anomalous pattern is seen clearly. When the threshold is set at M 3.0, the limit of the homogeneity of the list, the pattern is still observed, yet the anomaly becomes relatively indistinct. If we count aftershocks as small as M 0, we will not discover the quiescence because the occurrence of a small earthquake may reflect physical conditions of a small area which are often irrelevant to the preparation of a large earthquake. It is likely that the larger an aftershock is, the more affected its occurrence is by preparatory processes for the forthcoming large shock.

The b-value of the Gutenberg-Richter formula significantly changed at Q and R. In (10), the b-value of aftershocks of $M\geq 3.0$ calculated for each stage by the maximum likelihood method (UTSU, 1965) is shown with a 95% confidence interval (AKI, 1965).

$$b=\begin{cases} 0.72\pm 0.06 & T_0<t\leq Q \\ 1.30\pm 0.35 & Q<t\leq R \\ 0.81\pm 0.28 & R<t<T_1 \end{cases} \qquad (10)$$

The b-value increased after Q, which is equivalent to the fact that the frequency of larger aftershocks decreased more in the quiescent stage. After R, the b-value decreased to its original value.

Hypocenters in the area concerned cannot be located properly by usual methods, because the area is far from the network, the azimuthal coverage of the network is very narrow, S phases are not clear, and the accuracy of P-arrival times is often not good. Therefore, a new method of hypocenter location (MATSU'URA, 1984) has been adopted in order to avoid an insignificant scatter of hypocenters due to inaccuracy of data and defects in the network coverage. This method makes full use of prior information and gives a consistent confidence region for an obtained hypocenter. In addition to data from the stations of the Dodaira Micro-

earthquake Observatory and other stations of the Earthquake Research Institute, arrival-time data of JMA stations in and around the Kanto district were used when they were found in the original register of JMA.

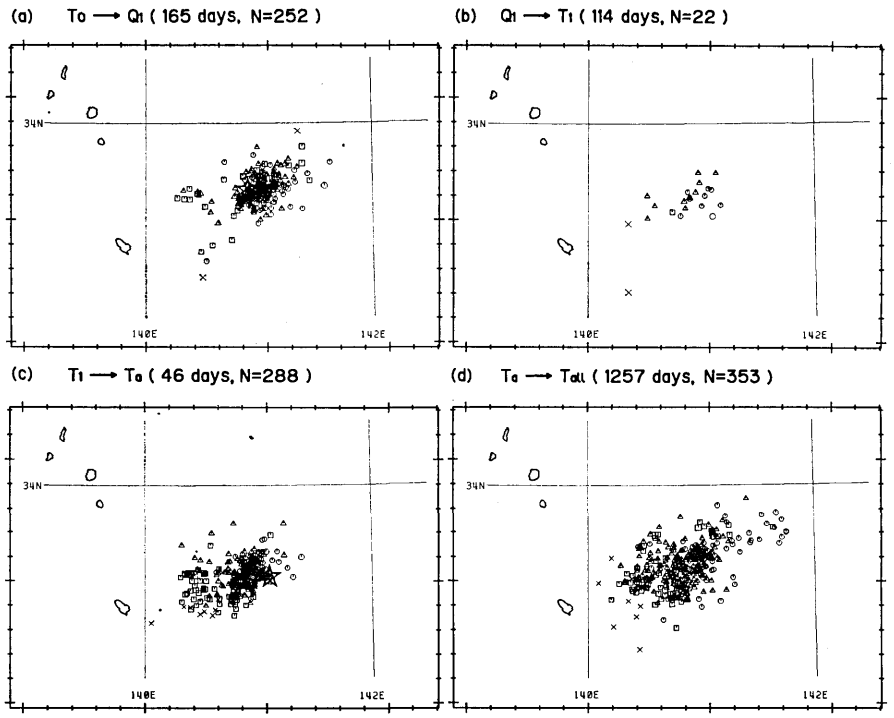

Fig. 5. The hypocenter distribution of $M \geq 3.5$ quakes in each stage. Octagons, triangles, squares, and crosses show hypocentral depths shallower than 30 km, 30 to 60 km, 60 to 90 km, and deeper than 90 km, respectively.

(a) Aftershocks of the first shock until the quiescence. The star indicates the hypocenter of the first shock.

(b) During the quiescence and the recovered stage. The open circle indicates the epicenter of the forthcoming second shock.

(c) For 46 days after the second shock. The star indicates the hypocenter of the second shock.

(d) From 46 days after the second shock until June 30, 1976.

All hypocenters of shocks of $M \geq 3.5$ are plotted in Fig. 5. In the quiescent and recovered stages, aftershocks occurred mostly near the hypocenters of the forthcoming second shock. After the second shock, aftershocks of the second shock occurred west of the aftershock zone of the first shock. Aftershocks of the first shock were also observed in the area active before Q.

ii) The western Nagano Prefecture earthquake of 1984

On September 14, 1984, Ohtaki Village near the western border of Nagano Prefecture was struck by a shallow earthquake of M_J 6.8. After one day, the largest aftershock of M_J 6.2 occurred on a fault conjugate to the main shock fault (Fig. 6). It disturbed the search for missing persons buried under the landslips caused by the main shock and frightened the local people. On October 3, 1984 and on February 26, 1985, rather large aftershocks of M_J 5.3 and M_J 5.0 occurred and were followed by their own aftershocks.

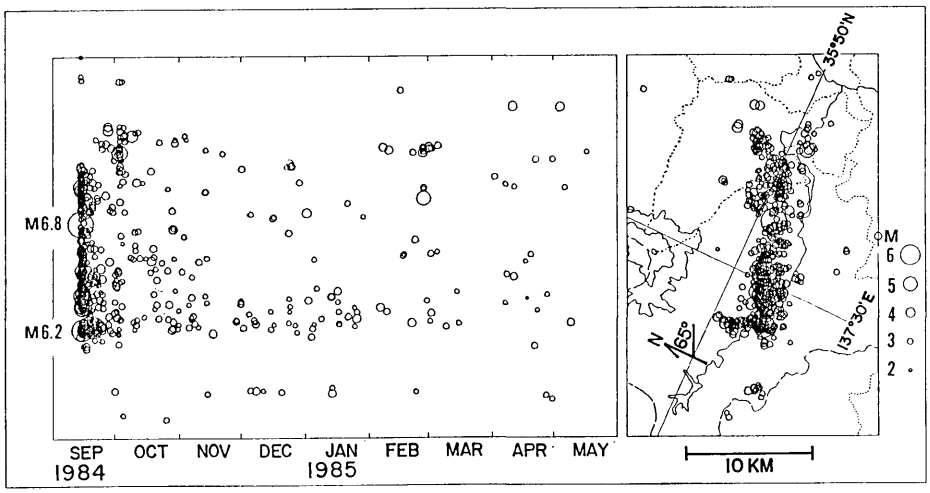

(After Mizoue et al., 1985)

Fig. 6. Epicenter distribution in the western part of Nagano Prefecture after MIZOUE *et al.* (1985). The N65°E lineament shows the fault of the main shock, while the conjugate short one shows the secondary aftershocks of the largest aftershock.

For studying this sequence, a list of aftershocks has been carefully made from the strip-chart type records of the Dodaira Microearthquake Observatory. Since the recorder was changed in 1983 to the thermal-pen type, which might cause a judgement of F-P time different from the previous recorder, constants in the formula relating the total duration time at the Dodaira station (DDR) to the magnitude by JMA are determined for this sequence as in the following.

$$M_J = 2.63 \cdot \log (\mathrm{F\text{-}P})_{\mathrm{DDR}} - 1.58 \qquad (11)$$

According to (11), the list is homogeneous for $M \geq 3.0$ except for the first ten minutes immediately following the onset of the main shock.

In the one-day interval from the main shock to the largest aftershock, the data deviate largely from the single modified Omori formula before the largest aftershock. In this case, the short quiescence and the following foreshock-like high activity are observed before the largest aftershock. When the (6-1)-type model is fitted to the sequence, the equal value of AIC to the (1)-type model (Fig. 7(a)) is achieved if $T_C=$ 0.6 day (Fig. 7(b)). As T_C increases, AIC decreases and p_0 value increases to an unusual value. When $T_C=0.74$ day (Fig. 7(c)), when the activity started to increase in Figure 7, the smallest AIC for the (6-1)-type model is obtained and p_0 becomes 2.86, which implies that the aftershock activity decreased with abnormal rapidity from 0.6 day to 0.74 day. Therefore, the (6-2)-type model with two discontinuities at Q and R is adopted. The smallest AIC for this model is obtained when $Q=0.6$ day, $R=0.74$ day, and

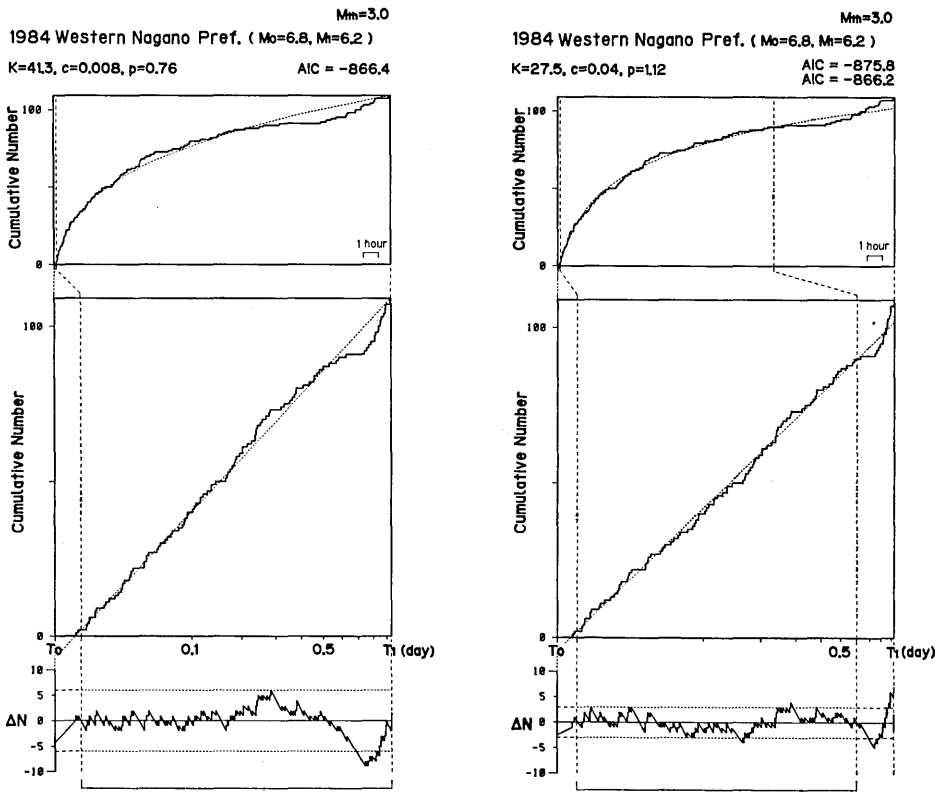

(a) (b)

Fig. 7.

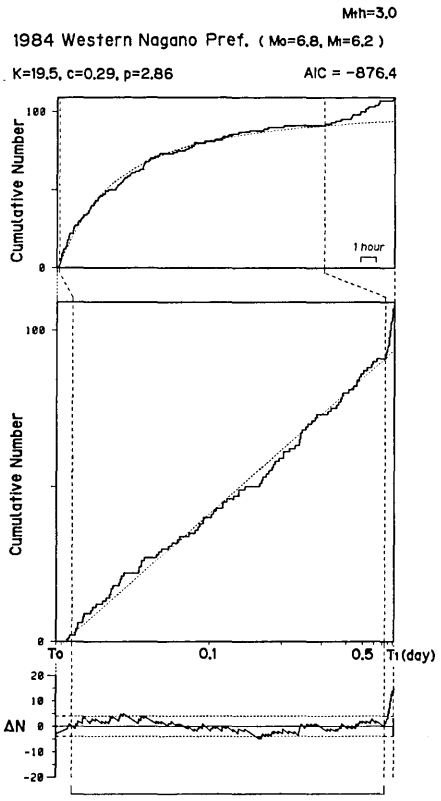

(c)

Fig. 7. Aftershock sequence of the western Nagano Prefecture earthquake during the period from the main shock to the largest aftershock.
(a) FLT from data for 10 min. $<t\leq T_1$.
(b) FLT from data until $t=0.6$ day. The smaller AIC value is that for the (6-2)-type model represented by (12). The other is that for the (6-1)-type model.
(c) FLT from data until $t=0.74$ day.

$$n(t)=\begin{cases}\dfrac{27.5}{(t+0.04)^{1.12}} & 0.007<t\leq Q\\ 7.1 & Q<t\leq R\\ 92.5 & R<t\leq T_1.\end{cases} \tag{12}$$

During the quiescence, the activity decreased one-fifth of the rate expected from the modified Omori formula for the normal aftershock activity before Q. In the recovered stage, the activity is three times as active as expected. Aftershocks located by MIZOUE *et al.* (1985) in this stage were distributed mostly near the forthcoming largest aftershock (Fig. 8). In the course of preparing the aftershock list, it was also noticed that

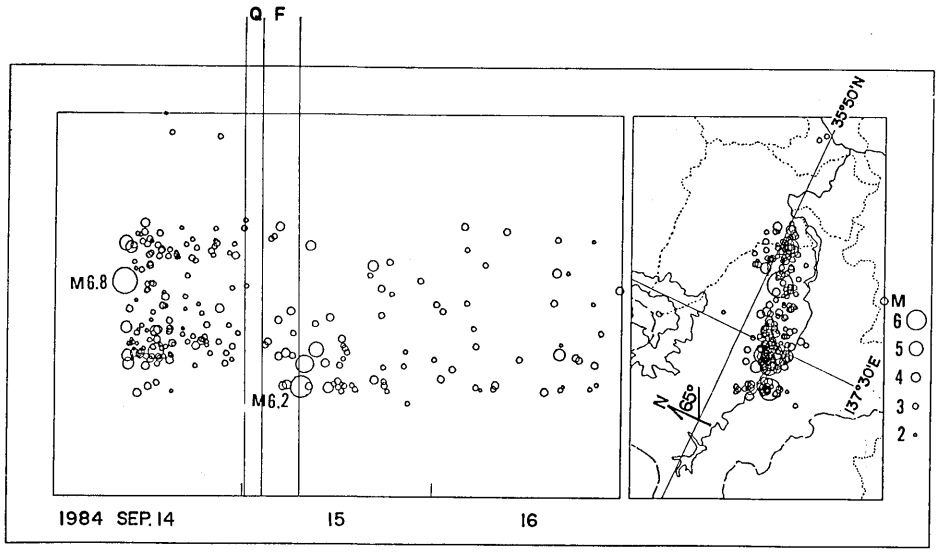

(Mizoue et al., 1985 with addition)

Fig. 8. Epicenter distribution in the western part of Nagano Prefecture after MIZOUE *et al.* (1985). *Q* and *F* indicate the beginning of the quiescence and the foreshock activity of the *M* 6.2 event.

a change in waveforms appeared before the largest aftershock. Before *R*, nearly equal ratios of the maximum *P*-wave amplitude to that of the *S*-wave at the DDR station were observed, while the different ratios were mixed in after *R*.

Before the other two large aftershocks, however, significant quiescence did not emerge (Figs, 9, 10). The large deviation from the modified Omori formula before the first shock with M_J 5.3 was due to the swarm-type activity on September 27 which occurred northeast of the east end of the main fault. The M_J 5.3 shock occurred on the eastward extension of the main fault. After this swarm activity, the aftershock activity returned to the rate expected from the modified Omori formula fitted to data before the swarm (Fig. 9). Eighteen hours before the shock, the activity increased slightly from the expected rate again without the preceding quiescent stage as for the largest aftershock. After this large aftershock, the degree of fluctuation from the modified Omori formula increased, which implies that the aftershock activity became rather intermittent after the M_J 5.3 earthquake (Fig. 10). Three months before the next large aftershock of M_J 5.0, the data were again well explained by the modified Omori formula of (7). The M_J 5.0 earthquake was preceded by a slight increase in activity for eight hours, although this foreshock

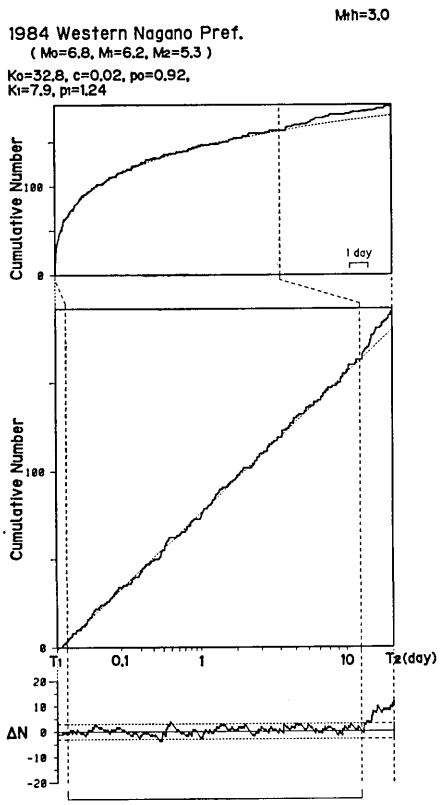

Fig. 9.

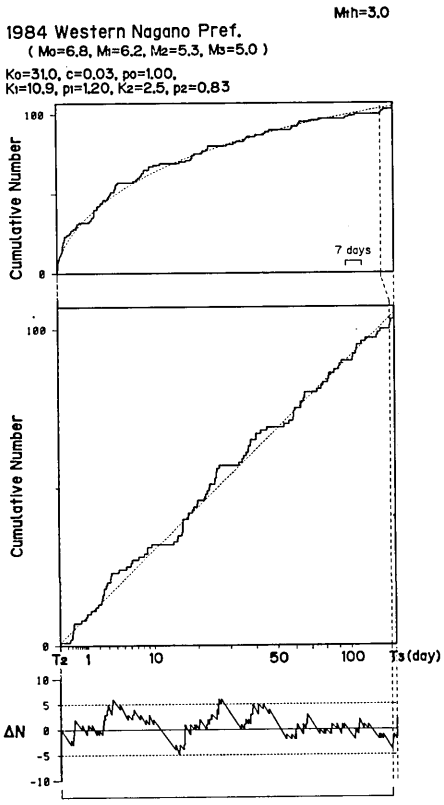

Fig. 10.

Fig. 9. Aftershock activities following the main shock and the largest aftershock for the time interval between the largest aftershock and the large aftershock of M_J 5.3 on Oct. 3. Parameters shown above are obtained from the data in the period from 10 minutes to 12 days after the largest aftershock (indicated by a square bracket) in addition to the data from 10 minutes to 0.6 day after the main shock.

Fig. 10. Aftershock activities of the main shock, the largest aftershock and the large aftershock of M_J 5.3 for the time interval between the large aftershock and the next large aftershock of M_J 5.0 on Feb. 26, 1985. Parameters are obtained from the data for the period 10 minutes to 141 days after the M_J 5.3 shock in addition to the data used for figure 9.

cluster did not produce a substantial change compared with the fluctuation in other periods. There was also no significant quiescent stage before this earthquake.

The explanation for the absence of significant quiescence in the aftershock activity before the two $M5$ aftershocks is that the lower limit of the present analysis ($M=3.0$) is too high to detect changes in these cases, or changes in physical conditions for preparation of an $M5$ earthquake are too small or affect too limited a zone to be noticeable in the activity

of the whole aftershock area. M 3.0 is the limit of detection at the DDR station for this area. At nearer stations operated by Nagoya University, ground noises from the construction of a path through nearby forests prohibited the sampling of smaller aftershocks homogeneously in daytime (AOKI, personal communication). Checking the former possibility is very difficult. However, the off Hachijo Island case implied that the chance of revealing the quiescent stage by including smaller aftershocks is very small. Therefore, the anomalous pattern of aftershock activity should be searched for before an aftershock which is not only followed by secondary aftershocks but also not smaller than the main shock by 1.5 unit of magnitude.

The Nagoya group (SCHOOL OF SCIENCE, 1985) reported that these three large aftershocks of the western Nagano Prefecture earthquake were all preceded by foreshocks a few hours earlier. They examined small aftershocks located within a zone of a few kilometers around the large aftershock for one day before it occurred. A cluster of activity emerged a few hours before in the small zone of the forthcoming large aftershock. However, a cluster of activity occurring in a limited zone does not always lead to a large aftershock in that zone. The cluster on September 27, large enough to be recognized in the activity of the whole area, was not followed by a large event. Some criteria to distinguish a mere cluster from a forerunner of an M 5 large aftershock should be searched for the purpose of prediction. For the largest aftershock, this study discriminates fluctuation from the foreshock activity of the largest aftershock with the quiescence.

iii) The Kanto earthquake of 1923

UTSU (1981) collected old instrumental and macroseismic data and made a homogeneous list of hypocenters ($M \geq 5.4$) for central Japan from 1904 to 1925. In this list, the largest earthquake is the great Kanto earthquake in 1923 with M_S 8.2 (M_U 7.9). Although the magnitude threshold of the catalog is much larger than in the previous two cases, the main shock is great enough to be followed by enough aftershocks to apply the present method. This earthquake was followed by the off Katsuura earthquake of M_S 7.7 (M_U 7.3) one day later, and the large aftershock of M_U 7.3 136 days later in Tanzawa. These cases are investigated.

In the aftershock sequence before the off Katsuura earthquake, the quiescent and recovered stages are clearly observed (Fig. 11(a)). The smallest AIC is obtained for the model with $Q=0.2$ day, $R=0.45$ day, and

$$n(t)=\begin{cases} \dfrac{5.2}{(t+0.07)^{1.62}} & T_0<t\leq Q \\ 0.0 & Q<t\leq R \\ 10.5 & R<t\leq T_1. \end{cases} \tag{13}$$

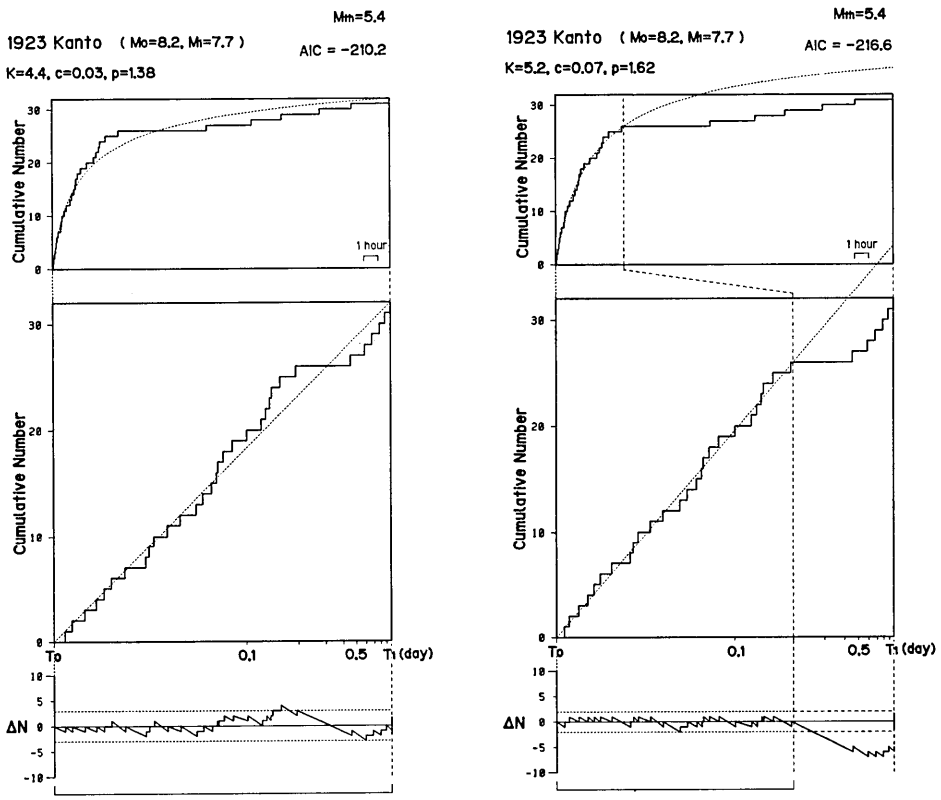

(a) (b)

Fig. 11. The aftershock sequence of the great Kanto earthquake until the occurrence of the off Katsuura earthquake.
(a) FLT from all data.
(b) FLT from data until $t=0.2$ day.

In this case, no aftershock of $M \geq 5.4$ occurred for six hours after the normal aftershock activity of five hours from the main shock (Fig. 11(b)). This complete quiescence is followed by a recovered aftershock activity. Epicenters of aftershocks (Fig. 12) in the recovered stage are mostly distributed in the southeast part of the main shock's source region, which is close to the forthcoming off Katsuura earthquake (Fig. 12(b)).

For the period after the off Katsuura earthquake, the activity is not just the combination of two aftershock sequences, although we exclude earthquakes which apparently occurred outside the source region. The smallest AIC for the whole activity from the main shock to the Tanzawa earthquake is achieved by

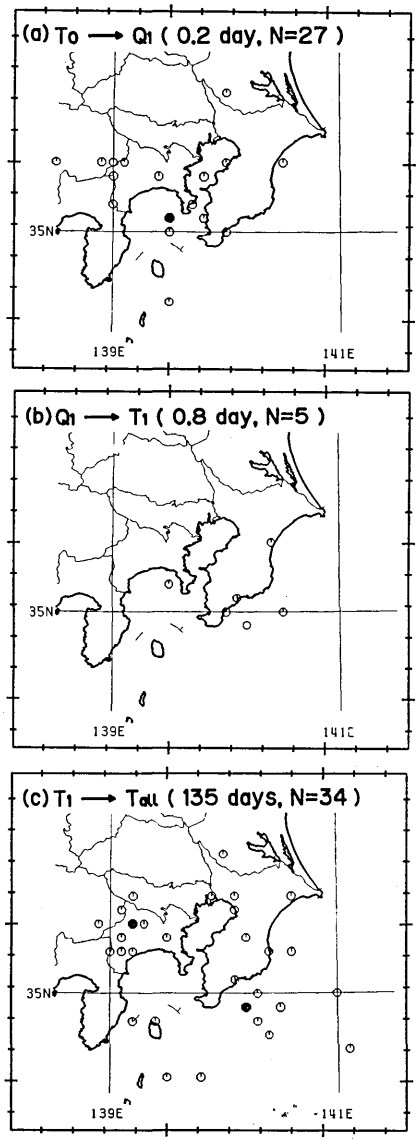

Fig. 12. Epicenter distribution of $M \geq 5.4$ in each stage for the aftershock sequence of the great Kanto earthquake. Solid circles show epicenters of the Kanto, the off Katsuura, and the Tanzawa earthquakes. An open circle in the middle figure shows the epicenter of the off Katsuura earthquake.

$$n(t)=\begin{cases}\dfrac{9.4}{(t+0.06)^{1.32}}+H(t-T_1)\cdot 0.1 & T_0<t\leq Q \text{ or } t>T_1\\ 0.0 & Q<t\leq R\\ 10.5 & R<t\leq T_1\end{cases} \tag{14}$$

where T_1 is the origin time of the off Katsuura earthquake. The occurrence rate after the off Katsuura earthquake is the summation of the aftershock activity of the main shock and an additional activity independent of the lapse time from the off Katsuura earthquake. There is no large deviation in data of this period from (14) (Fig. 13).

After the great Kanto earthquake, the seismicity in the Kanto district decayed slowly as pointed out by OHNAKA (1984) and taken into account in OGATA and KATSURA (1986). The constant term added after T_1 represents this. A great earthquake of M 8 disturbs the asthenosphere

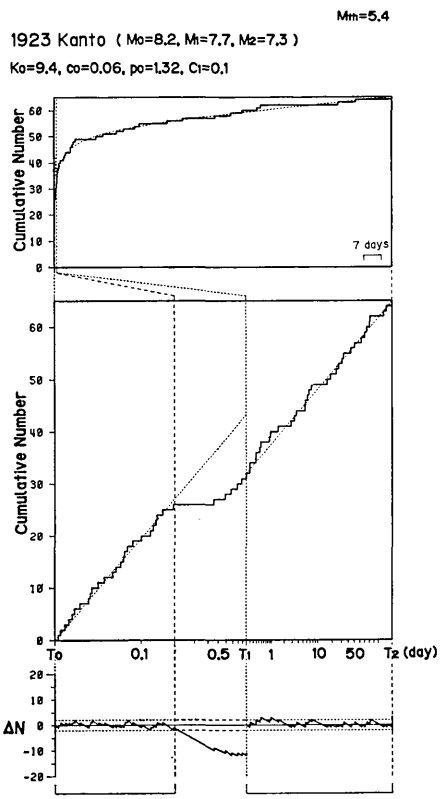

Fig. 13. The aftershock sequence during the period from the great Kanto earthquake to the Tanzawa earthquake. The parameter $C_1=K_1$ when $p_1=0$. After T_1, figures under the frequency-linearized time axis show the lapse time from T_1 instead of T_0.

(e.g. MATSU'URA *et al.*, 1981); thus it activates a wide area, creates aftershocks which are only caused by a great earthquake and decay very slowly due to the viscoelastic relaxation in the asthenosphere. The one-day interval between the main shock and the off Katsuura earthquake is too short to distinguish aftershocks peculiar to a great earthquake from ordinary aftershocks, and the four-month interval before Tanzawa earthquake is not long enough to reveal the slow decay of those particular aftershocks. The aftershock activity of the off Katsuura earthquake is too weak compared to the activity induced by the deformed asthenosphere due to great Kanto earthquake. It appears as a small upward deviation for three days from T_1 in Figure 13.

The Tanzawa earthquake may be smaller than the off Katsuura earthquake, although it had the same magnitude as the off Katsuura earthquake in the catalog by UTSU (1981). Its surface wave magnitude was not obtained from worldwide data (ABE, personal communication). There are no aftershocks of $M \geq 5.4$ for the Tanzawa earthquake, while there are some for the off Katsuura earthquake. The magnitude of this earthquake may be overestimated in the Utsu catalog, probably because it occurred on land and released most energy at high frequencies.

However, quiescence and recovery might be revealed in the activity before the Tanzawa earthquake, if we could distinguish ordinary aftershocks from earthquakes induced by the viscoelatic relaxaton in the asthenosphere. They might also be recognized if a catalog of small magnitude threshold like $M4$ or $M3$ were available. The inclusion of small aftershocks might result in putting stress on the ordinary aftershock activity. The data available tell us that changes in the aftershock activity due to the preparetion of a large aftershock tend to be unrecognized when activities due to other factors are involved.

5. Results obtained from somewhat inhomogeneous data sets

i) The Niigata earthquake of 1964

In order to investigate whether the emergence of quiescence and recovered activity in an aftershock sequence before a large aftershock is universal, it is necessary to analyze as many sequences as possible with published catalogs. For sequences in and around Japan, the Seismological Bulletin of JMA is most useful. However, the homogeneity of JMA catalogs is not guaranteed. The degree of deviation in the JMA catalog from the modified Omori formula for a normal aftershock sequence without a large aftershock should be checked before it is used for further analysis.

The aftershock activity of the Niigata earthquake which occurred on June 16, 1964 with M_S 7.5 ($=M_J$) is the best example of normal aftershock activity. This earthquake occurred just offshore northern Niigata Prefecture and many aftershocks were located by the JMA network. Its largest aftershocks were only M_J 6.1. Secondary aftershock activities were scarcely observed even by the temporal nearby observation of aftershocks (THE PARTY FOR AFTERSHOCK OBSERVATION, 1968). No expansion of the aftershock area was recognized for this earthquake (MOGI, 1968a). If the JMA data of this sequence had any large deviation from the modified Omori formula, they would be unusable for detecting activity changes in an aftershock sequence.

All aftershocks located by the JMA network are used for analysis regardless of their magnitudes given in the bulletin (Fig. 14). The limit of homogeneity for a catalog is often obtained by drawing Gutenberg-Richter's diagram. The lowest limit of magnitude is chosen as a bending point where a cumulative number curve of earthquakes starts to deviate

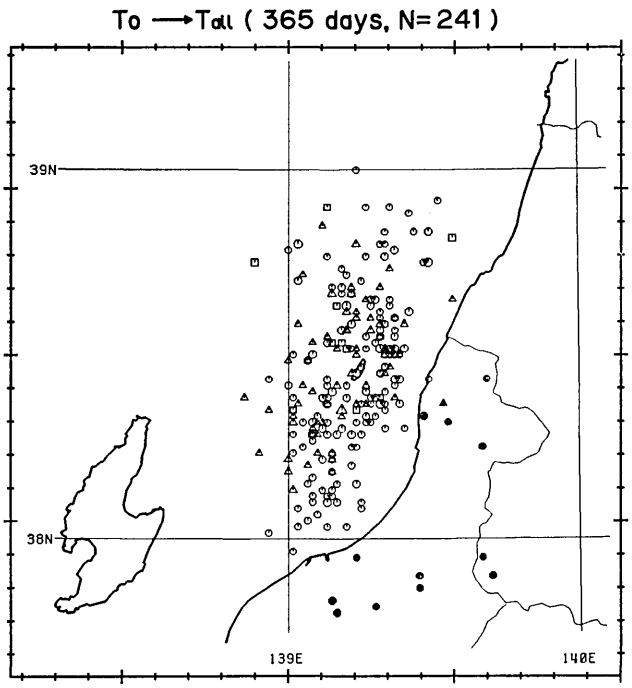

Fig. 14. Hypocenter distribution of the Niigata earthquake and its aftershocks for one year afterwards. (Earthquakes indicated by solid circles and a solid triangle are excluded from the analysis, because they are located outside the focal area. However, including those earthquakes does not affect the results.) For symbols, see the caption in Figure 5.

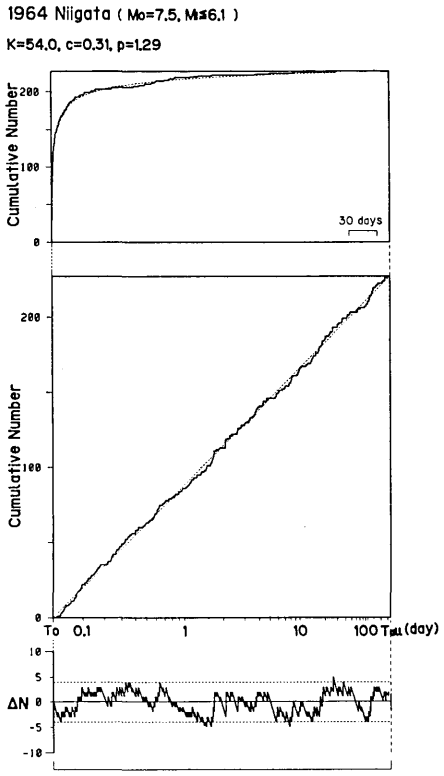

Fig. 15. The aftershock sequence of the Niigata earthquake for one year.

from the Gutenberg-Richter formula. This threshold is M 4.0 for the Niigata sequence from the list in a special report (JMA, 1965). However, tentative magnitudes are assigned to more than half of the aftershocks in this list without using sufficient data. The magnitude columns for those earthquakes are blank in the bulletin. An aftershock large enough to be located by the JMA network is considered above a certain threshold held uniform through this old sequence.

This aftershock sequence is expressed by the modified Omori formula very well (Fig. 15). The standard deviation of data from the formula is very small. There is no period of remarkable deviation as seen in sequences having large aftershocks. AIC for the (1)-type model is smaller than the AIC for the (6-1)-type model; in other words, there is no anomalous change of activity in this sequence. Hereafter, data in the JMA bulletin are used for further study.

ii) The off Miyagi Prefecture earthquake of 1978

On June 12, 1978, an M_S 7.5 (M_J 7.4) earthquake occurred offshore

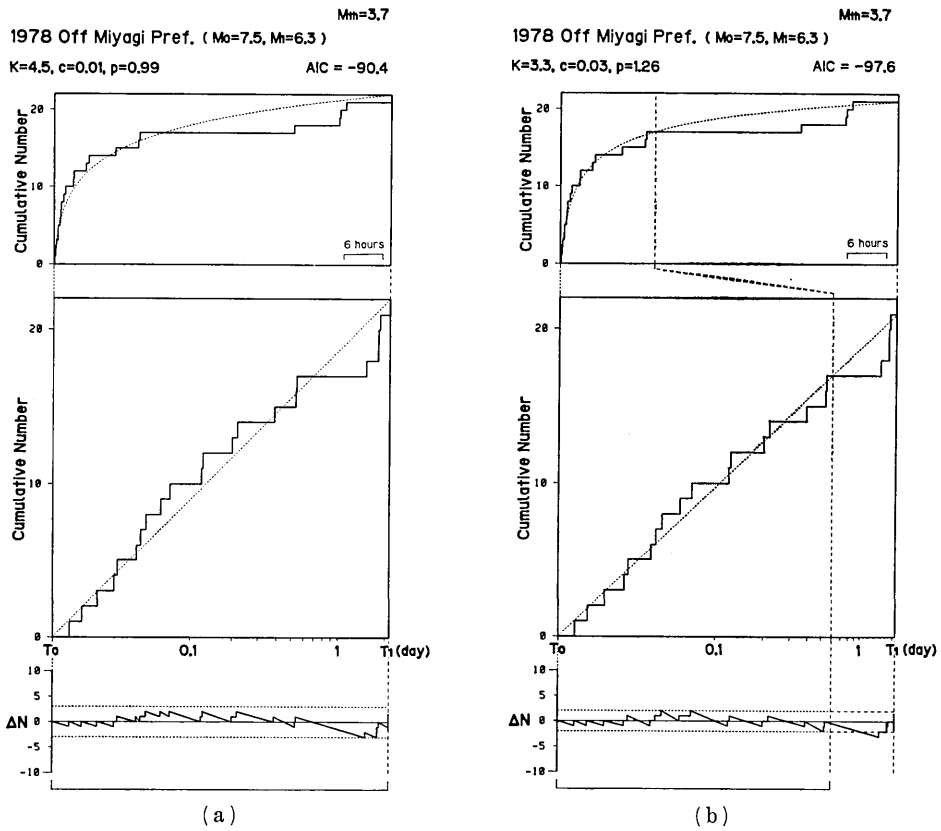

(a) (b)

Fig. 16. The aftershock sequence of the off Miyagi Prefecture earthquake during the period from the main shock to the largest aftershock.
(a) FLT from all data.
(b) FLT from data until $t=0.6$ day.

from Sendai city. The largest aftershock of M_J 6.3 followed two days later. The magnitude threshold of JMA data for this sequence is obtained as M 3.7 from Gutenberg-Richter's diagram.

Although the number of aftershocks is small, quiescence and the recovered activity are evidently recognized before the largest aftershock (Fig. 16 (a)). The smallest AIC is obtained for

$$n(t)=\begin{cases}\dfrac{3.3}{(t+0.03)^{1.26}} & T_0<t\leq Q\\ 0.0 & Q<t\leq R\\ 7.8 & R<t\leq T_1\end{cases} \tag{15}$$

where $Q=0.6$ day and $R=1.5$ day (Fig. 16 (b)). Most of the recovered activity is observed in the easten part of the main fault which is close

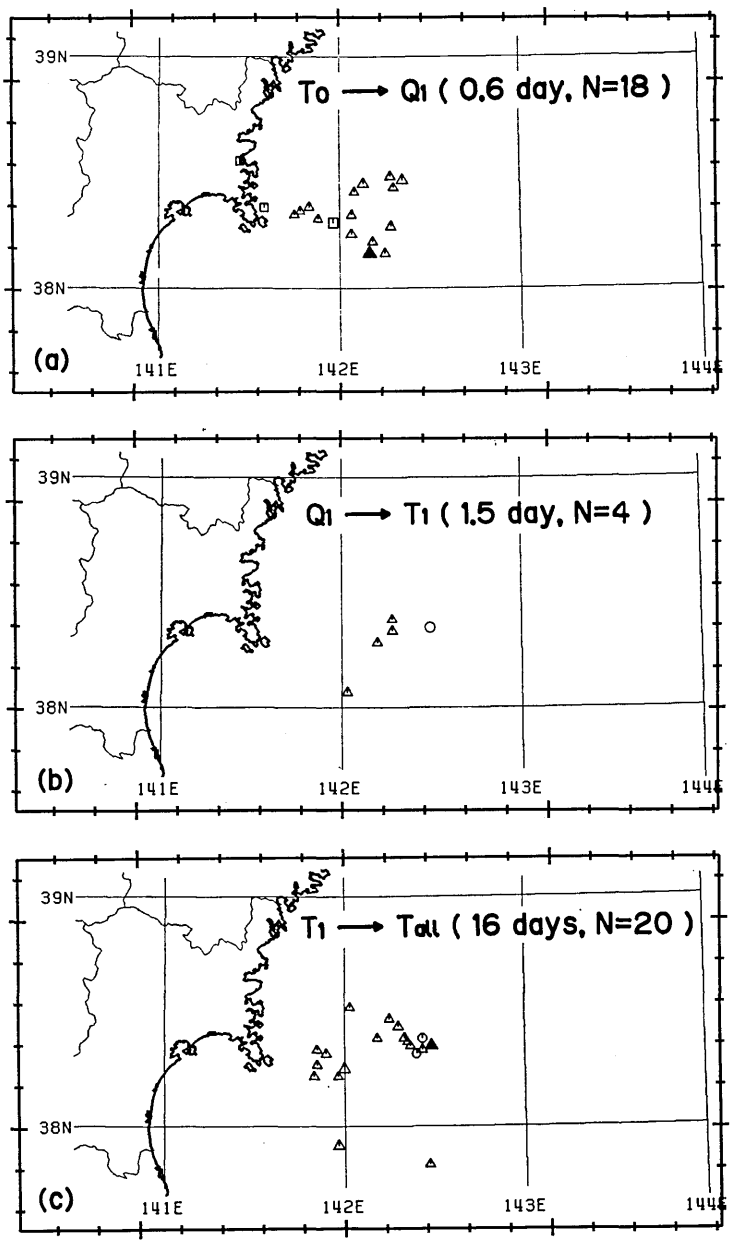

Fig. 17. The hypocenter distribution of the off Miyagi Prefecture earthquake and its aftershocks of $M \geq 3.7$. For symbols, see the caption in Figure 5.
(a) From the main shock (the solid triangle) to the quiescence.
(b) From the quiescence to the largest aftershock (the open circle).
(c) From the largest aftershock (the solid triangle) to June 30, 1978.

to the site of the forthcoming largest aftershock (Fig. 17).

Although the number of events analyzed is small, the peculiar variation in the activity before the largest aftershock can be regarded as a precursor, since it is far more anomalous than the fluctuation of the activity after the largest aftershock (Fig. 18 (a)). If we analyze only aftershocks which occurred in the source region of the main shock, the sequence after the largest aftershock is represented well by the summation of the aftershock activities of the main shock and the largest aftershock. The quiescent and recovered stages before the largest aftershock are significant through the whole sequence.

However, by including the activity in the area east of the main shock's source region (Fig. 19), an activity which may have been induced by the main shock, the sequence is not well represented by the modified

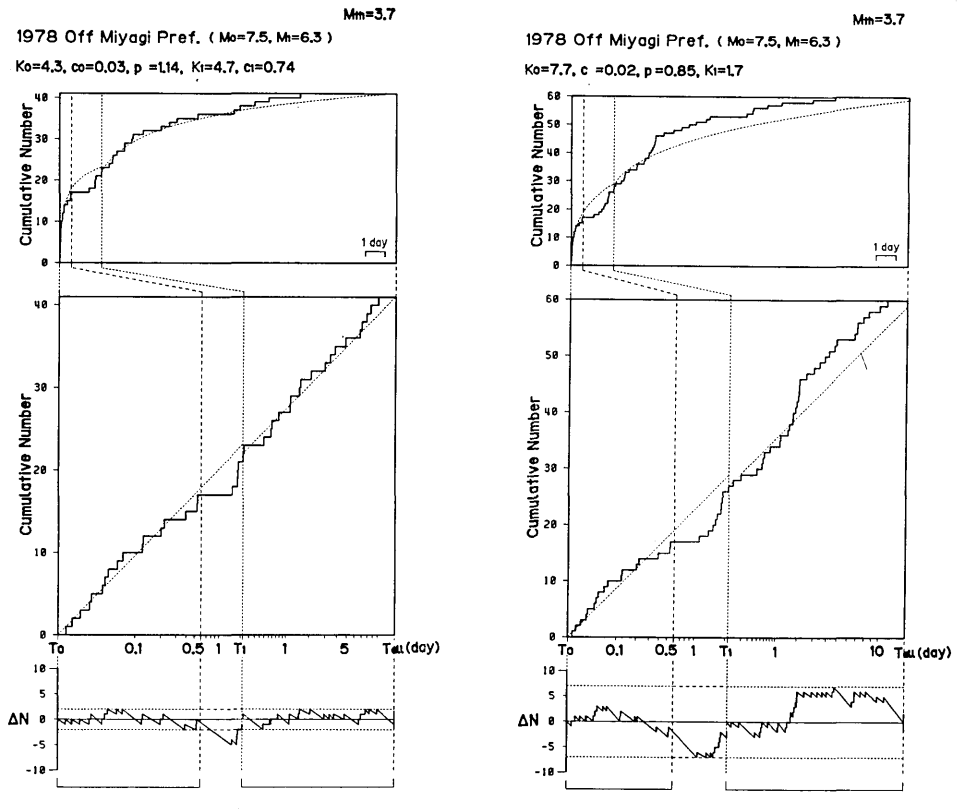

(a) (b)

Fig. 18. The aftershock sequence of the off Miyagi Prefecture earthquake during the period from the main shock until June 30, 1978.
(a) Earthquakes in the focal area shown in Figure 17.
(b) Earthquakes in the wider area shown in Figure 19.

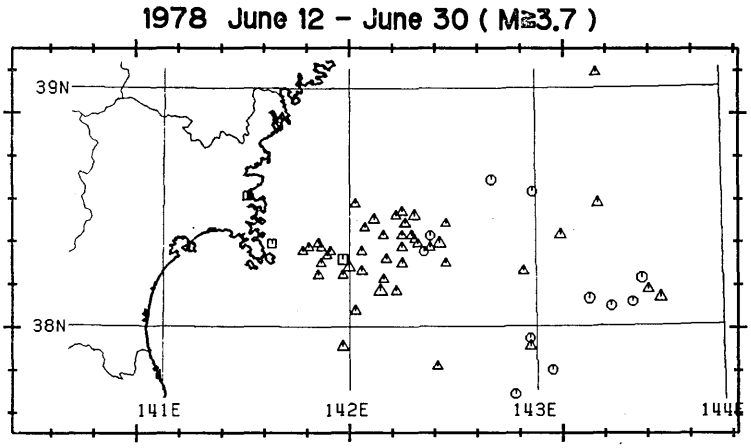

Fig. 19. The Hypocenter distribution of earthquakes of $M \geq 3.7$ located within the shown area in the same period as Figure 17.

Omori formula (Fig. 18 (b)). The modified Omori formula represents aftershock activity in the main shock area. After a large earthquake, there are not only aftershocks of this kind but also induced activities. The disturbance in the asthenosphere induces the particular activity after a great earthquake as in the great Kanto earthquake sequence. Static deformations in the surrounding areas also induce activities after a large earthquake. Those are usually not large but enough to cause failures in areas having already reached critical conditions before the occurrence of the main shock. The occurrence rate of such induced activities is controlled by factors other than the lapse time from the main shock. When the main shock occurs near an area in critical condition, discriminating true aftershocks from earthquakes due to other factors becomes very important for the present analysis.

iii) The Japan Sea earthquake of 1983

On May 26, 1983, an M_J 7.7 earthquake occurred off Akita Prefecture and many lives were lost in tsunami. On June 9, a pair of M_J 6.1 and 6.0 aftershocks occurred 14 minutes apart near the southern end of the source region of the main shock. This pair was followed by its own aftershocks. On June 21, the largest aftershock of M_J 7.1 occurred near the northern end of the source region of the main shock and it was also followed by many aftershocks. These sequences are analyzed using data of $M \geq 4.0$ in the JMA catalog.

The sequence from the main shock until the southern events is not explicable by a simple aftershock activity in the form of (1) (Fig. 20 (a)). There are some effects from the breakdown of the nearest high-sensitivity station of JMA in Aomori for three hours after the main shock. However,

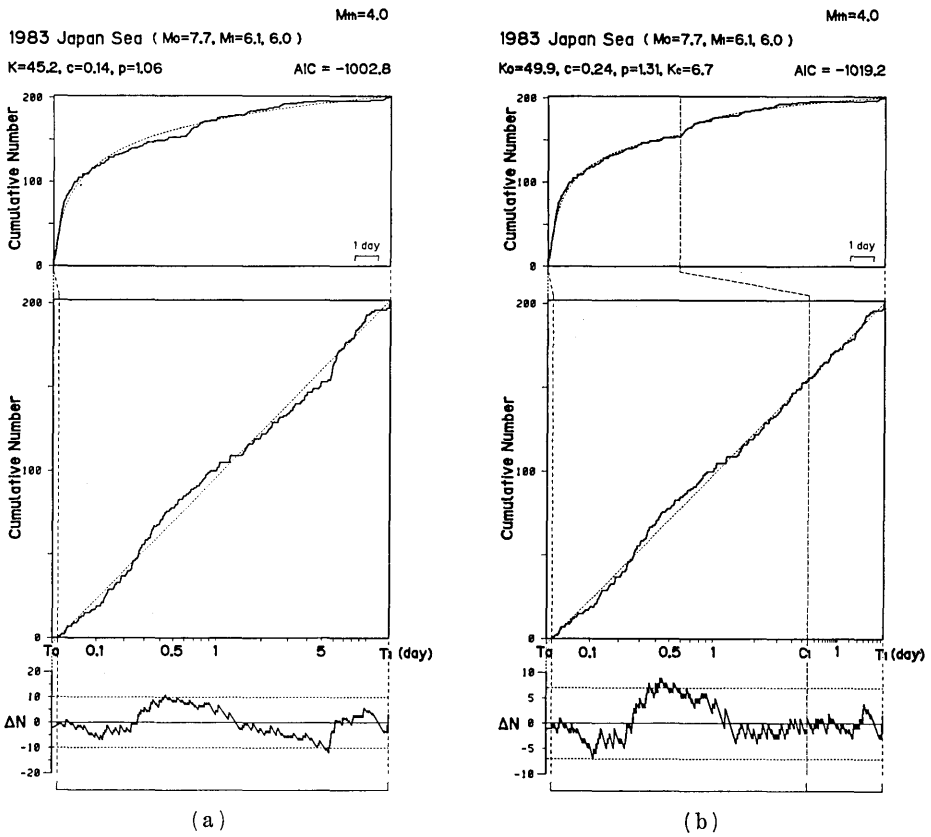

Fig. 20. The aftershock sequence of the Japan Sea earthquake until the two large southern aftershocks.
(a) FLT for the (1)-type model.
(b) The secondary aftershock activity is introduced at C_1=5.6 day when a cluster activity started.

the largest deviation started on June 1. On this day, aftershocks of M 5.1 and 5.2 occurred successively at the bend of the aftershock area of the main shock where the M 6.1 aftershock occurred one hour after the main shock. Two M 5.1 aftershocks also occurred near the hypocenter of the main shock on June 1. The increase of activity on June 1 was not a secondary aftershock activity of one large event. It did not cause the expansion of the aftershock area. However, this extra activity is approximated by introducing the modified Omori formula starting at the origin time of the first M 5.1 earthquake (C_1 in Figures 20 (b) and 21) in this cluster (Fig. 20 (b)).

Even when the cluster is taken into account, the activity from 0.2 day to 0.4 day is still more intense than expected. There was no large

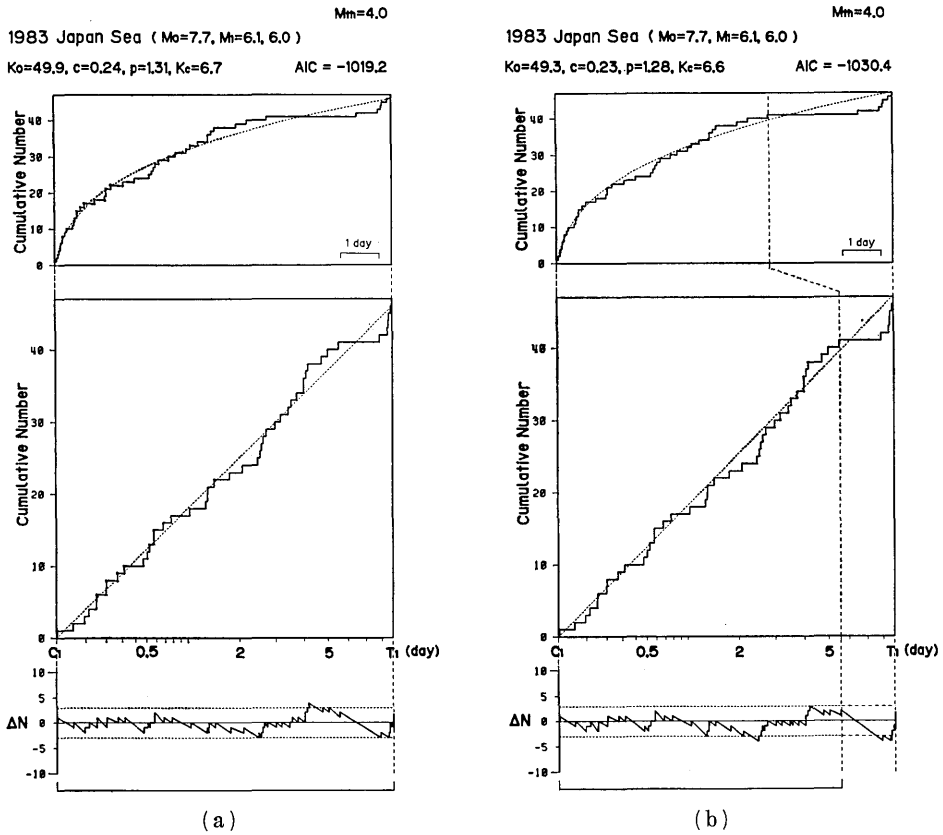

(a) (b)

Fig. 21. The aftershock sequence of the Japan Sea earthquake during the period from the cluster to the southern events. Parameters are determined from data in the range shown at the bottom in addition to data from 15 minutes after the main shock to the start of the cluster. Values of p and c are chosen in common for the mainshock and the cluster, since they give the smallest AIC.
(a) FLT from all data.
(b) FLT from data until t=11.2 day.

event around that time. During that period, M 4.0 aftershocks occurred successively, while M 3 aftershocks were mixed with M 4 in other periods. There is a possibility that the procedure of magnitude determination changed slightly at the period. After that period, the deviation of data is small except for the period before the southern events.

The southern events, which are equivalent to a single M 6.25 earthquake in energy, were preceded by quiescence and recovered activity (Fig 21 (a)). The smallest AIC is obtained for

$$n(t)=\begin{cases}\dfrac{49.3}{(t+c)^p}+H(t-C_1)\cdot\dfrac{6.6}{(t-C_1+c)^p} & 0.01<t\leq Q_1\\ 0.0 & Q_1<t\leq R_1\\ 6.6 & R_1<t\leq T_1\end{cases} \tag{16}$$

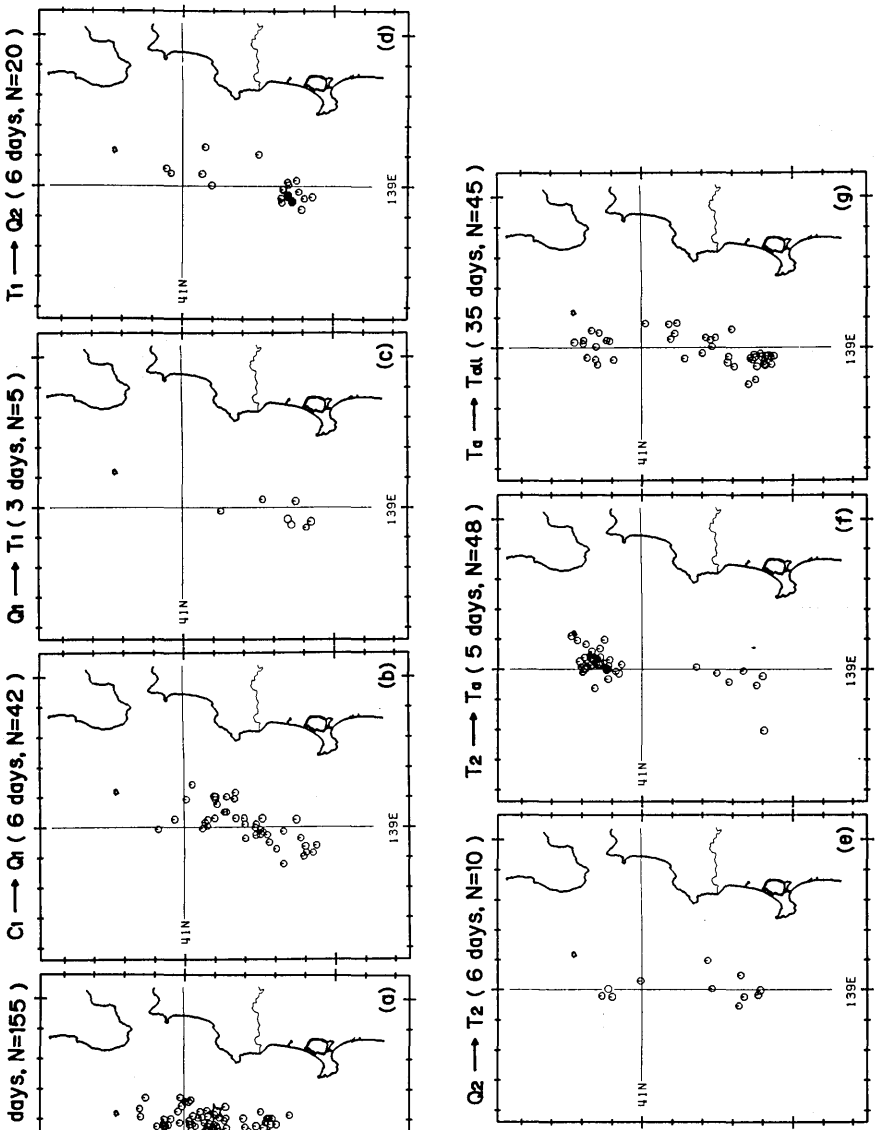

Fig. 22. The hypocenter distribution of the Japan Sea earthquake and its aftershocks of $M \geq 4.0$. For symbols, see the caption in Figure 5.
(a) From the main shock (the solid star) to the cluster. The M 6.1 aftershock that occurred one hour after the main shock is also shown by the open star. (b) From the cluster to the quiescence before the southern events. (c) From the quiescence to the southern events shown by open circles. (d) From the southern events (solid circles) to the quiescence before the largest aftershock. (e) From the quiescence to the largest aftershock shown by the open circle. (f) For five days from the largest aftershock (the solid circle). (g) Until the end of July 1983.

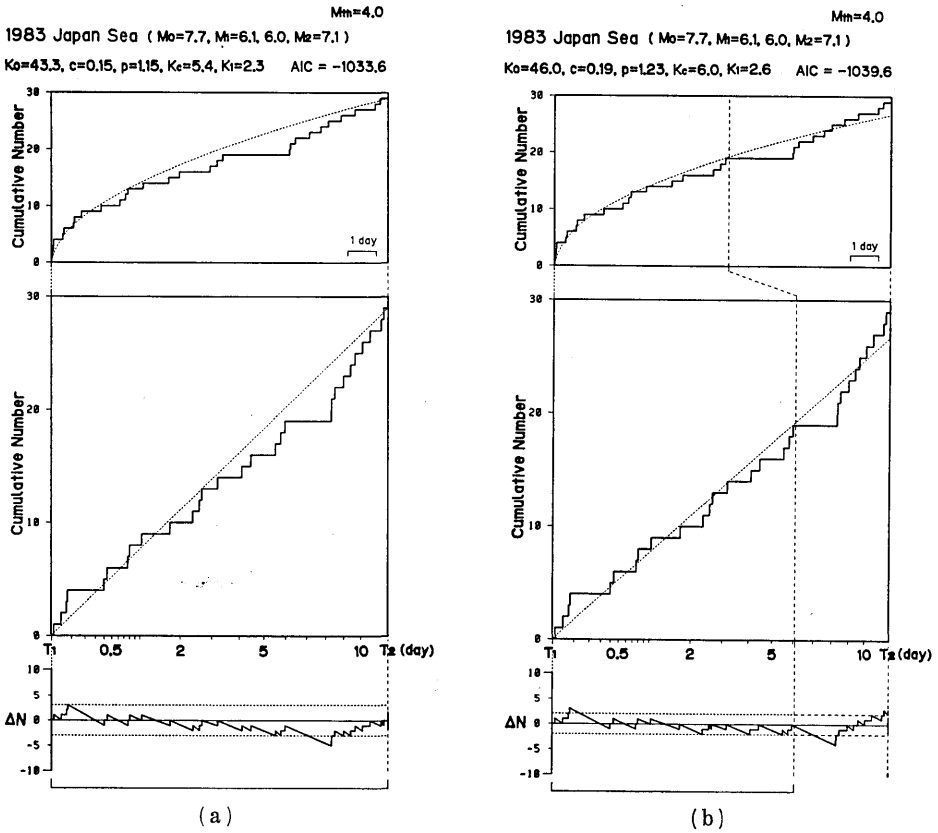

Fig. 23. The aftershock sequence of the Japan Sea earthquake during the period from the southern events to the largest aftershock. Parameters are determined from data in the range shown at the bottom in addition to data used for Figure 21(b). Values of p and c are chosen in common for three activities to obtain minimum AIC.
(a) FLT from all data shown here in addition to those used for Figure 21(b).
(b) FLT for the first equation of (17).

where $c=0.23$, $p=1.28$, $Q_1=11.2$ day, and $R_1=13.5$ day (Fig. 21 (b)). Aftershocks in the recovered stage were mainly distributed near the forthcoming southern events (Fig. 22 (a)-(c)).

Before the largest aftershock, quiescence and recovered activity also emerged (Fig. 23 (a)). The smallest AIC is obtained for

$$n(t)=\begin{cases}\dfrac{46.0}{(t+c)^p}+H(t-C_1)\cdot\dfrac{6.0}{(t-C_1+c)^p}+H(t-T_1)\cdot\dfrac{2.6}{(t-T_1+c)^p} & \\ & 0.01<t\leq Q_1 \text{ or } T_1<t\leq Q_2 \\ 0.0 & Q_1<t\leq R_1 \text{ or } Q_2<t\leq R_2 \\ 6.6 & R_1<t\leq T_1 \\ 3.0 & R_2<t\leq T_2\end{cases} \tag{17}$$

where $c=0.19$, $p=1.23$, $Q_2=20.5$ day $R_2=22.5$ day (Fig. 23 (b)). In this recovered stage, the middle part of the aftershock area was quiescent again. Instead the activity appeared at the northern end which had been quiet (Fig. 22 (d), (e)). However, there were also some aftershocks in the southern end which must be secondary aftershocks of the southern events. In this case, it was difficult to predict at which end the next large aftershock would take place.

iv) The off Takachi earthquake of 1968

On May 16, 1968, the off Tokachi earthquake of M_S 8.1 (M_J 7.9) occurred. Ten hours later, the largest aftershock of M_S 7.7 (M_J 7.5) occurred near the northern end of the source region. On June 12, another large aftershock of M_S 7.3 (M_J 7.2) occurred south of the source region.

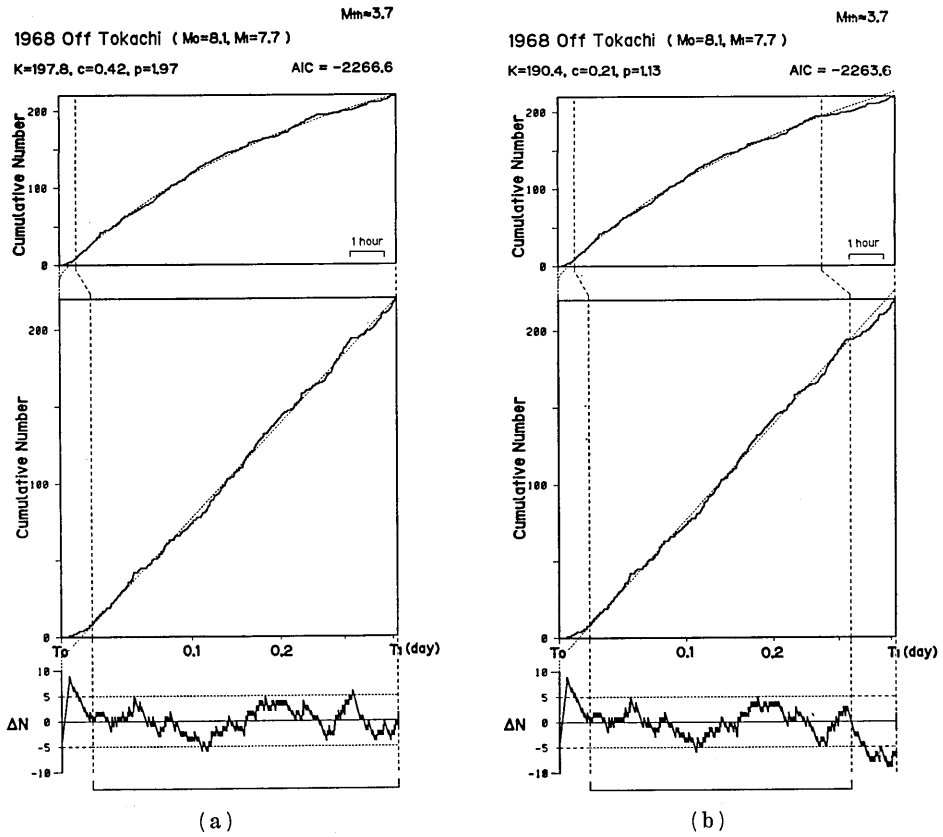

Fig. 24. The aftershock sequence of the off Tokachi earthquake during the period from the main shock to the largest aftershock. The data for the first thirty minutes are excluded from the estimation of parameters.
(a) FLT from all data.
(b) FLT from data until $t=0.32$ day.

It is called the off Iwate earthquake. Since this sequence was a remarkable one, a rather careful list of hypocenters of earthquakes of M 4.5 or over was published by JMA (1969). However, this list is apparently inhomogeneous for a few hours after major earthquakes.

For the sequence between the main shock and the largest aftershock, the list of felt and unfelt earthquakes of JMA is used instead of the list of hypocenters. There were only ten hours between the two earthquakes. The number of located aftershocks is too small for the present analysis even if the inhomogeneous period of the list is included. If the b-value of the Gutenberg-Richter formula is assumed as one, the calculated threshold for this list becomes about M 3.7.

Before the largest aftershock, there are a decrease and recovery of

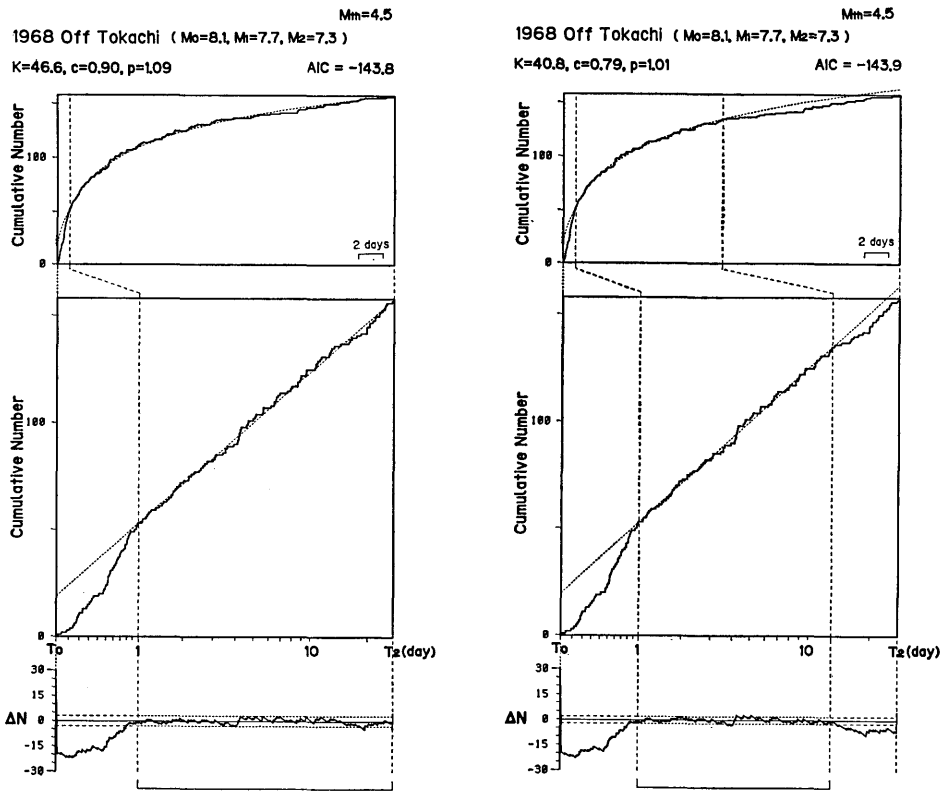

Fig. 25. The aftershock sequence of the off Tokachi earthquake during the period from the main shock to the off Iwate earthquake. The data for the first day are excluded from the estimation of parameters.
(a) FLT from data until T_2.
(b) FLT from data until t=13 days.

activity. However, these changes are not so prominent in comparison with the deviations in other periods, AIC for the (1)-type model (Fig. 24 (a)) is smaller than for the (6-1)-type model (Fig. 24 (b)) and the (6-2)- and (6-3)-type models, although the values of p and c for the (1)-type model are rather unusual.

This list of earthquakes has some defects for use in the present analysis. It contains only observed or felt times of earthquakes by the minute instead of origin times by the second. For the period of small t, more accurate origin times of aftershocks are required for our analysis. The list does not contain magnitudes for each earthquake. Earthquakes in the list are categorized into five ranks: remarkable, moderate, small felt area, local, and unfelt. These ranks are based on the size of the felt area and are not always related to magnitude. Aftershocks were not sampled evenly for this sequence. If the homogeneous list of origin

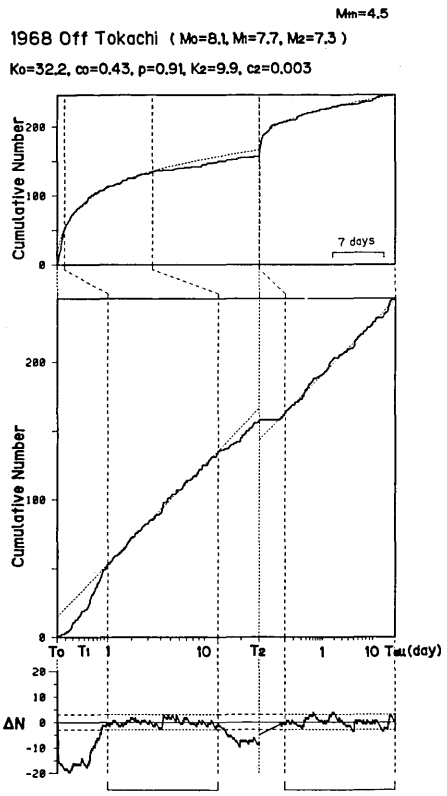

Fig. 26. The aftershock sequence of the off Tokachi earthquake till June 30, 1968. The p value is common to the main shock and the off Iwate, while c values are estimated for each. Data for one hour right after the off Iwate earthquake are not used for the estimation of parameters.

times were available, the quiescence before the largest aftershock might become significant.

For analyzing the sequence before the off Iwate earthquake, the list of hypocenters is used. The sequence is the combination of the aftershock activities of the main shock and the largest aftershock. However, these two activities cannot be separated, because the data within a few hours after the main shock and the largest aftershock are excluded and the two major events occurred at a short time interval. The sequence is treated as the aftershock of a single event at the time of the main

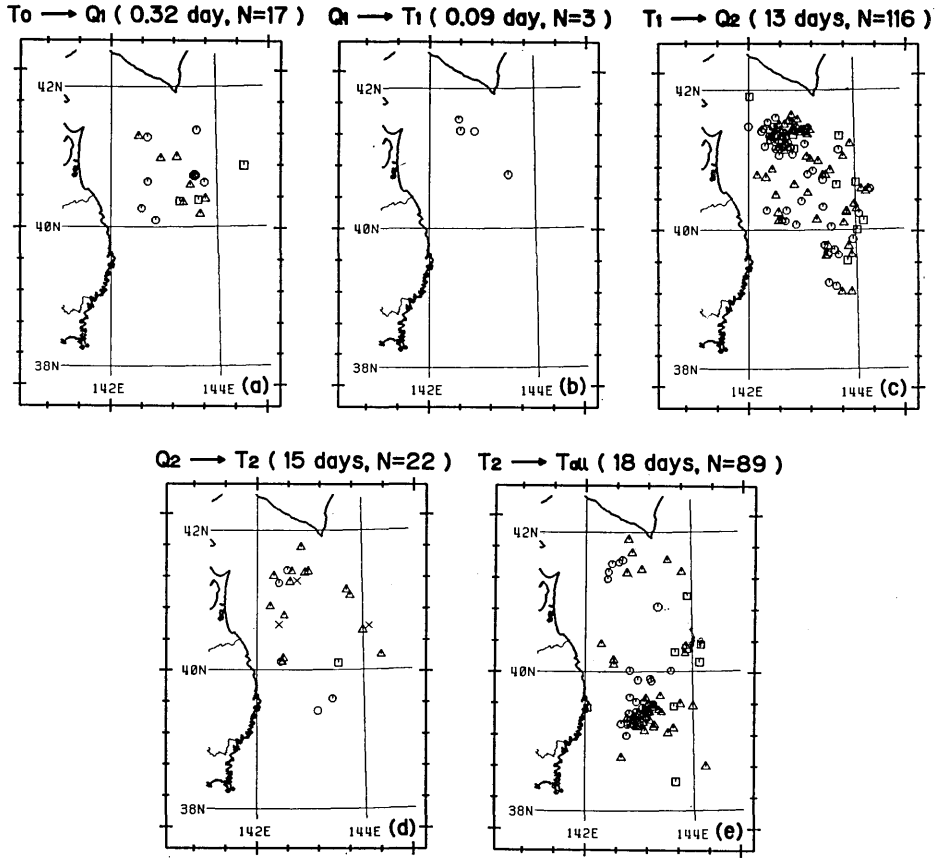

Fig. 27. The hypocenter distribution of the off Tokachi earthquake and its aftershocks of $M \geq 4.5$. For symbols, see the caption in Figure 5.

(a) From the main shock (the solid circle) to the quiescence before the largest aftershock.

(b) From the quiescence to the largest aftershock (the open circle).

(c) From the largest aftershock to the quiescence before the off Iwate earthquake.

(d) From the quiescence to the off Iwate earthquake (the open circle).

(e) From the off Iwate earthquake to June 30, 1968.

shock. Instead data within one day from the main shock are not used.

Before the off Iwate earthquake, there is significant quiescence (Fig. 25 (a)). The smallest AIC is obtained for

$$n(t)=\begin{cases}\dfrac{40.8}{(t+0.79)^{1.01}} & 1<t\leq Q_2, \quad R_2<t\leq T_2\\ 1.1 & Q_2<t\leq R_2\end{cases} \tag{18}$$

where $Q_2=13$ days and $R_2=19.5$ day (Fig. 25 (b)). However, AIC does not decrease greatly when Q_2 and R_2 are introduced, since the difference in the rate between the quiescence and the recovered stage is small.

The sequence after the off Iwate earthquake is used to check the validity of ignoring the use of different equations for the two aftershock sequences following the main shock and the largest aftershock. The whole

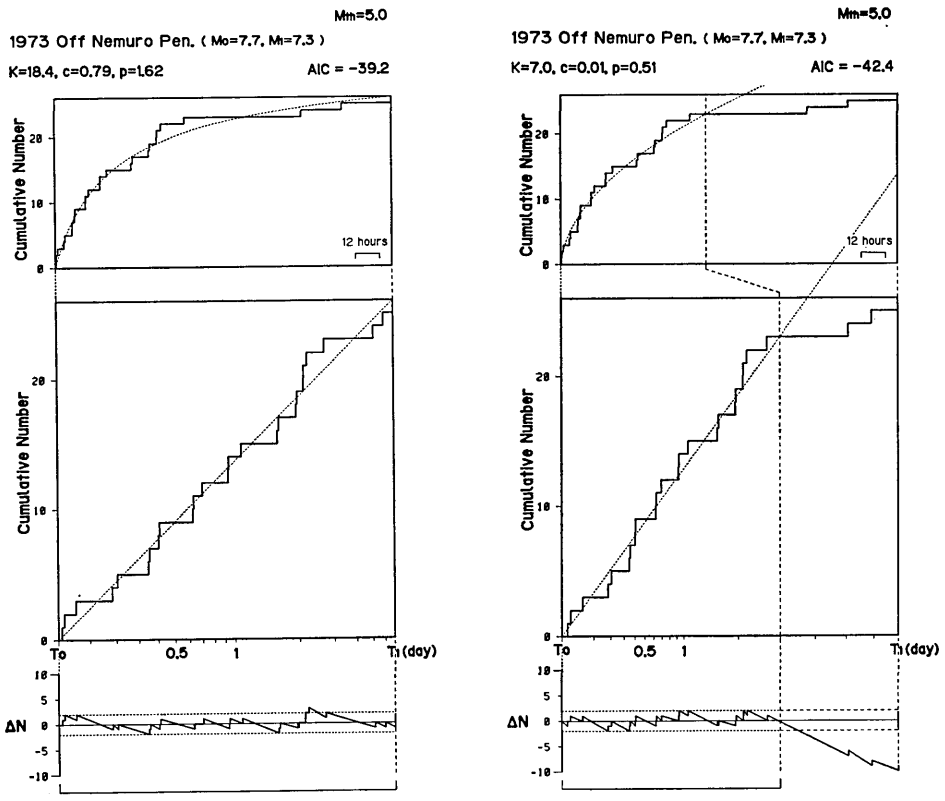

(a) (b)

Fig. 28. The aftershock sequence of the off Nemuro Peninsula earthquake during the period from the main shock to the largest aftershock.
(a) FLT from all data.
(b) FLT from data until $t=3$ days.

sequence from the main shock until June 30 can be represented by combining the aftershock activities of the main shock and the off Iwate earthquake, except for the period before the off Iwate earthquake (Fig. 26). There is no large deviation in periods without large aftershocks.

The hypocenter distribution in the quiescent period before the largest aftershock suggests the location of the forthcoming largest aftershock (Fig. 27 (b)), while the hypocenter of the off Iwate earthquake cannot be predicted from the activity after the second quiescence (Fig. 27(d)). In the bulletin of JMA, however, smaller earthquakes of about M 4 located in the region off Iwate increased in number from the beginning of June.

v) The off Nemuro Peninsula earthquake of 1973

On June 17, 1973, an M_S 7.7 (M_J 7.4) earthquake occurred off the

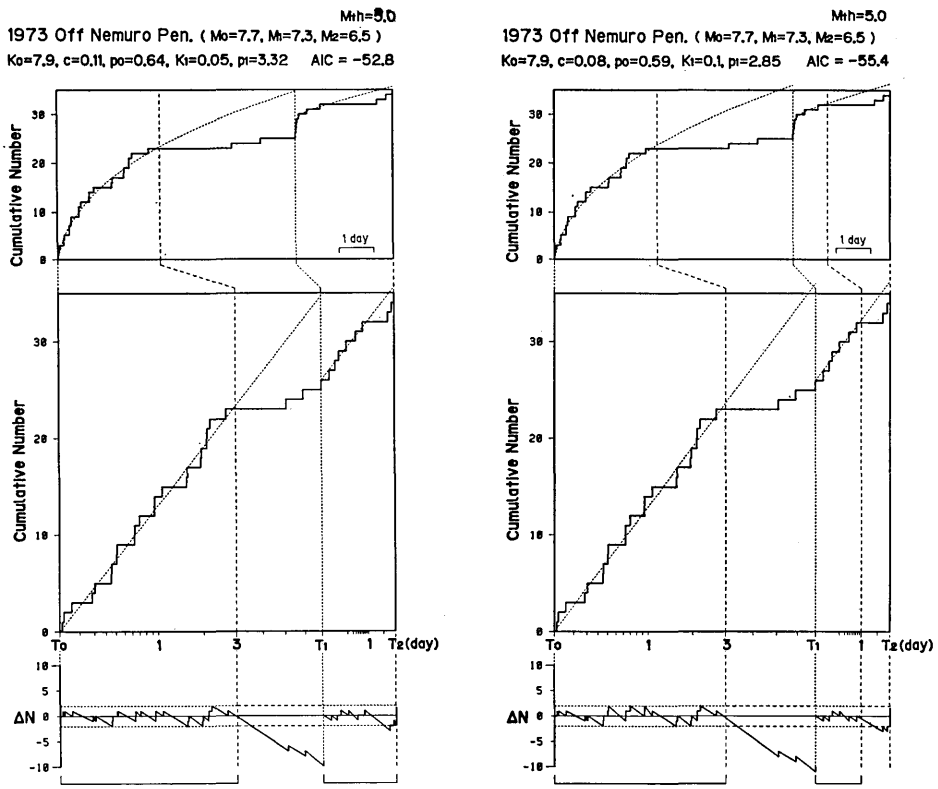

(a) (b)

Fig. 29. The aftershock sequence of the off Nemuro Peninsula earthquake during the period from the main shock to the second largest aftershock. The c-value is chosen in common for the two activities to obtain minimum AIC.

(a) FLT from all data except those in the anomalous period before the largest aftershock.

(b) FLT from data until t=8 days.

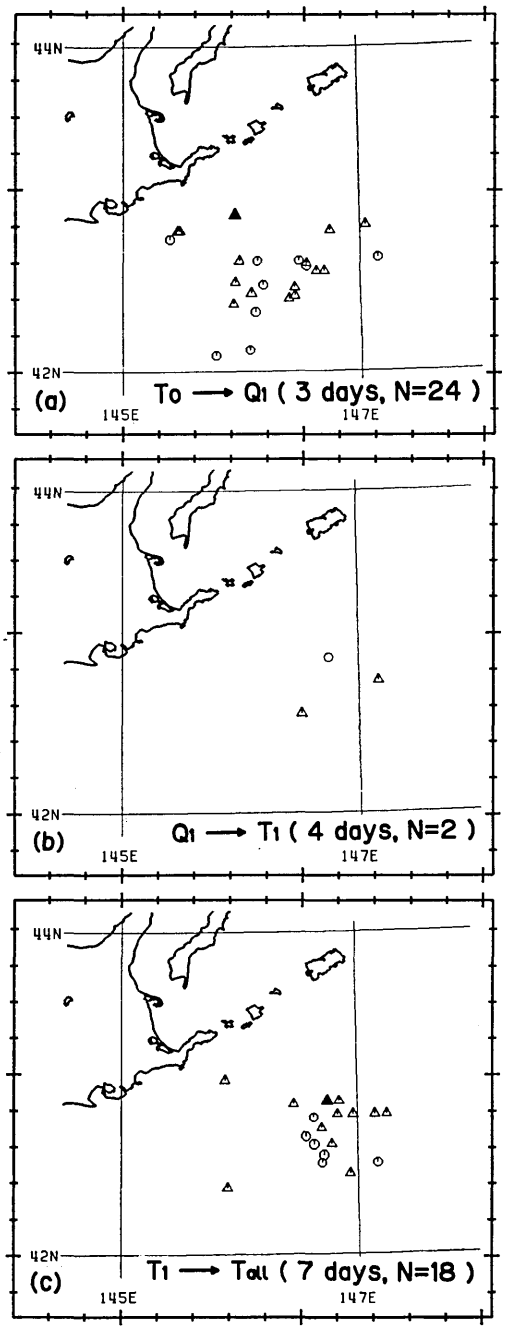

Fig. 30. The hypocenter distribution of the off Nemuro Peninsula earthquake and its aftershocks of $M \geq 5.0$. For symbols, see the caption in Figure 5.
(a) From the main shock (the solid triangle) to the quiescence.
(b) From the quiescence to the largest aftershock (the open circle).
(c) From the largest aftershock (the solid triangle) to June 30, 1973.

Nemuro Peninsula, where a seismic gap had been pointed out (UTSU, 1970). On June 24, a quake of M_S 7.3 (M_J 7.1) followed it near the eastern end of the source region. Not only this largest aftershock, but also the second largest aftershock of M_J 6.5 on June 27 was followed by secondary aftershocks. The limit of homogeneity of the hypocenter list of JMA for this sequence is M 5.0. This large threshold is due to the absence of JMA stations on the islands east of Hokkaido.

Before these large aftershocks, the activity decreased significantly and then recovered (Figs. 28, 29). Similar changes were visible in the daily frequency figures of felt earthquakes at Nemuro and at Kushiro before the largest aftershock (JMA, 1974), but were not evident before the second largest. In the recovered stage before the largest aftershock, aftershocks again occurred near the hypocenter of the forthcoming largest aftershock (Fig. 30 (b)).

vi) The off Iturup Island earthquake of 1963

On October 13, an M_S 8.1 ($=M_J$) earthquake occurred off Iturup Island. This earthquake was preceded by a large foreshock of M_S 7.0 (M_J 6.3) eighteen hours earlier. The largest aftershock occurred on October 20 with M_S 7.2 (M_J 6.7) and the second largest aftershock of M_J 6.2 occurred on November 16 (Fig. 31). These two large aftershocks caused

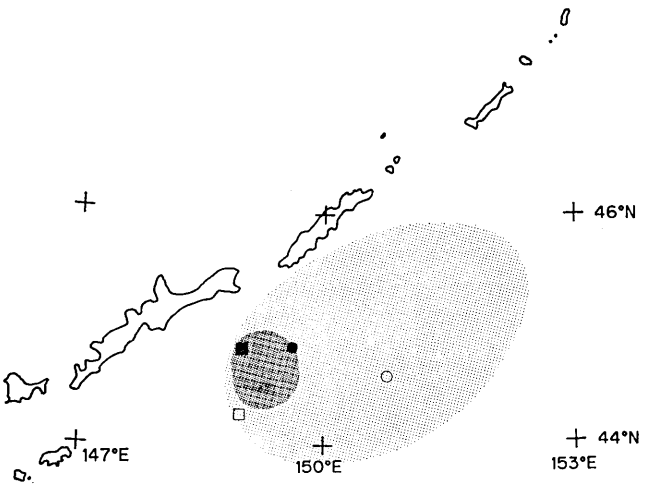

Fig. 31. The source region of four major shocks of the off Iturup Island sequence of 1963. Lightly and heavily dotted areas show the aftershock areas of the main shock and the largest foreshock, respectively. Closed and open circles and squares show the epicenter of the main shock, the largest aftershock, the largest foreshock, and the second largest aftershock, respectively.

the secondary aftershock activities. The activity after the large foreshock is also of an aftershock-type, obeying the modified Omori formula. Therefore, three cases of anomalies in aftershock activity can be investigated in this sequence.

This sequence is examined using the data compiled by SANTO (1964). He studied this sequence based on the preliminary epicenters determined by U. S. C. G. S. The data in his list are homogeueous for $M \geq 4.5$ on the basis of Gutenberg-Richter's diagram. Since the accuracy of hypocenters is not good, only the activitiy change is checked for this sequence.

In the aftershock activity following the large foreshock, we notice quiescence and recovery before the main shock (Fig. 32). However, the number of aftershocks is too small to check the statistical significance of those activity changes in this case. After the main shock, this aftershock activity of the foreshock still continued. AIC for the model including this activity is smaller than that of the model considering the

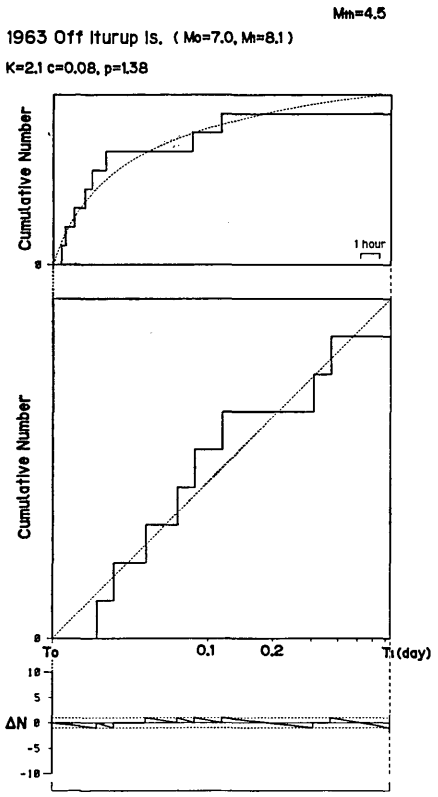

Fig. 32. The aftershock sequence of the largest foreshock of the off Iturup Island earthquake during the period from the largest foreshock to the main shock.

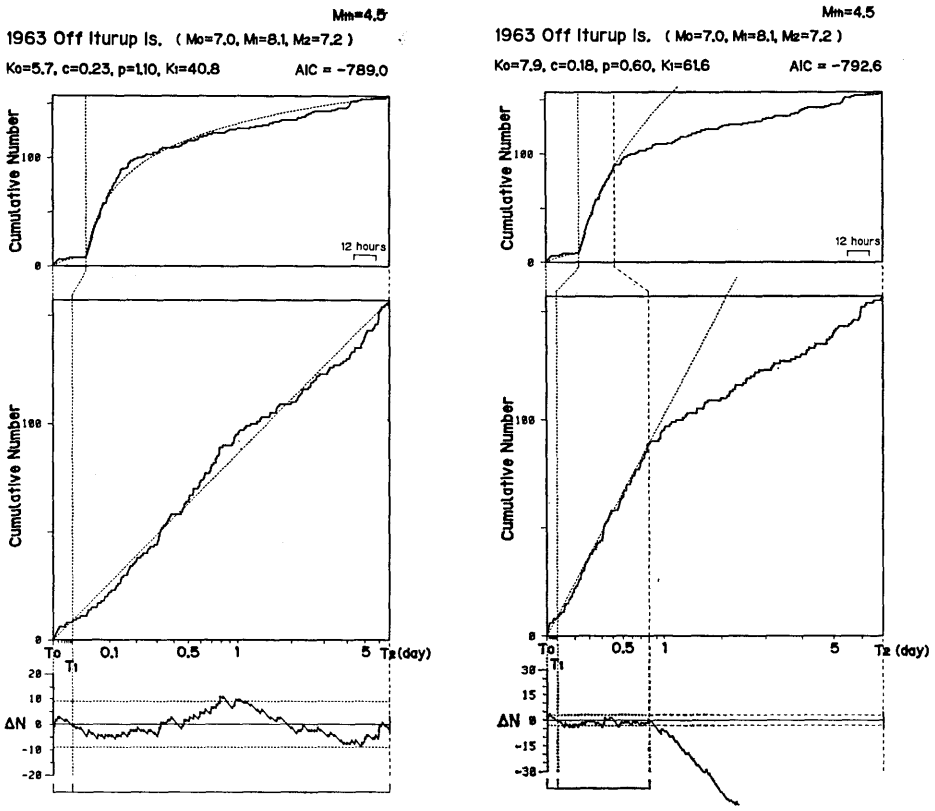

(a) (b)

Fig. 33. The aftershock sequence of the off Iturup Island earthquake and the largest foreshock during the period from the largest foreshock to the largest aftershock.
(a) FLT from all data.
(b) FLT for the first equation of (19).

aftershock activity of the main shock only.

The aftershock activity after the main shock decreased only 0.8 day later (Fig. 33 (a)). The smallest AIC is obtained for the (6-1)-type model as

$$n(t)=\begin{cases}\dfrac{7.9}{(t+c)^p}+H(t-T_1)\cdot\dfrac{61.6}{(t-T_1+c)^p} & T_0<t\leq Q_2\\[2ex] \dfrac{20.4}{(t-T_1)^{0.53}} & Q_2<t\leq T_2\end{cases} \tag{19}$$

where $c=0.18$, $p=0.60$, and $Q_2=T_1+0.8$ day (Fig. 33 (b)). Although the activity shows recovery five days later, that change is rather small and gradual. AIC for the (6-2)- or (6-3)-type model with $R_2=6.2$ day is

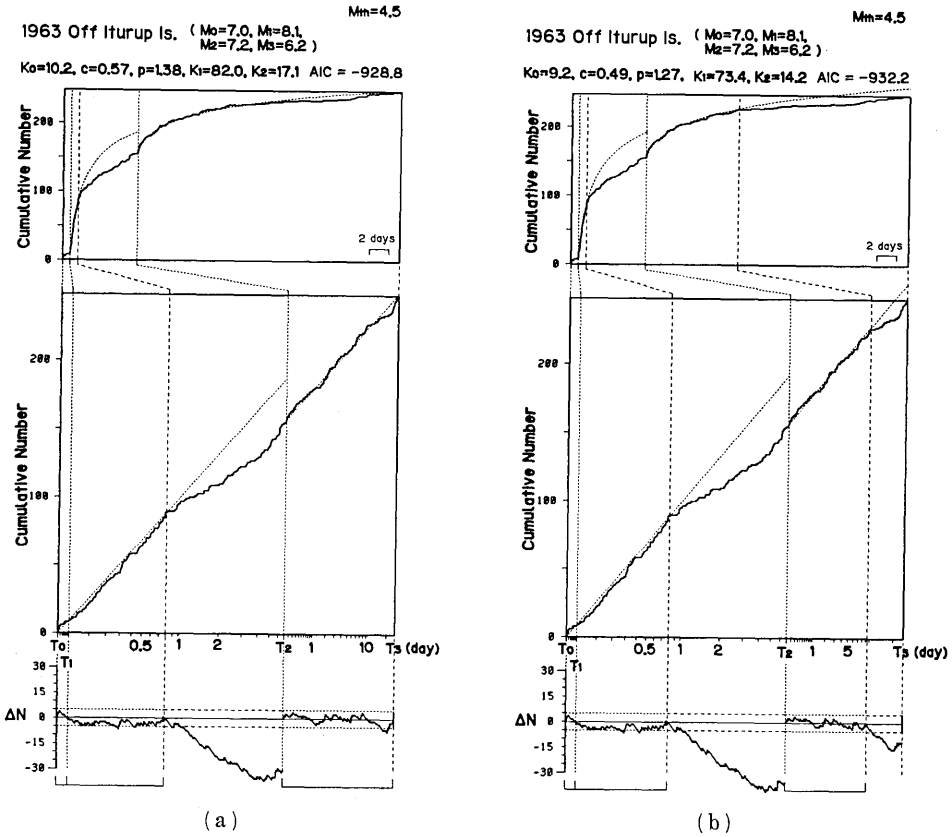

(a) (b)

Fig. 34. The aftershock sequence of the off Iturup Island earthquake, the largest foreshok, and the largest aftershock during the period from the largest foreshock to the second largest aftershock.

(a) FLT from all data except those in the anomalous period before the largest aftershock.

(b) FLT for the first equation of (20).

smaller than the (1)-type model, but not smaller than the model with Q only.

The activity before the second largest aftershock also shows a fall and then a rise (Fig. 34 (a)). The smallest AIC is for

$$n(t)=\begin{cases}\dfrac{9.2}{(t+c)^p}+H(t-T_1)\cdot\dfrac{73.4}{(t-T_1+c)^p}+H(t-T_2)\cdot\dfrac{14.2}{(t-T_2+c)^p} & T_0<t\leq Q_2 \text{ or } T_2<t\leq Q_3\\ \dfrac{20.4}{(t-T_1)^{0.53}} & Q_2<t\leq T_2\\ 0.8 & Q_3<t\leq R_3\\ 2.0 & R_3<t\leq T_3\end{cases} \tag{20}$$

where $c=0.49$, $p=1.27$, $Q_3=17$ days, and $R_3=29$ days (Fig. 34 (b)).

vii) The Tonakai earthquake of 1944

On December 7, 1944, the Tonakai earthquake of M_S 8.0 (M_J 7.9) took place southeast off the Kii Peninsula. On January 13, 1945, the Mikawa earthquake of M_S 6.8 ($=M_J$) occurred in the Atsumi Peninsula at the northeastern end of the source region of the Tonakai earthquake (Fig. 35). Many secondary aftershocks followed it. The Mikawa earthquake is famous for being preceded by remarkable foreshock activity. Deduced from results of this study, there must be a quiescent stage in the aftershock activity of the Tonakai earthquake before the foreshock activity of the Mikawa earthquake. However, there is no good list of hypocenters for this sequence. It occurred during the last stage of World War II, when seismological observations were confused and suffered from a shortage of recording paper, etc. The list of felt earthquakes in Geophysical Review of JMA is used for the analysis.

Our analysis focuses on whether the quiescence emerged befre the

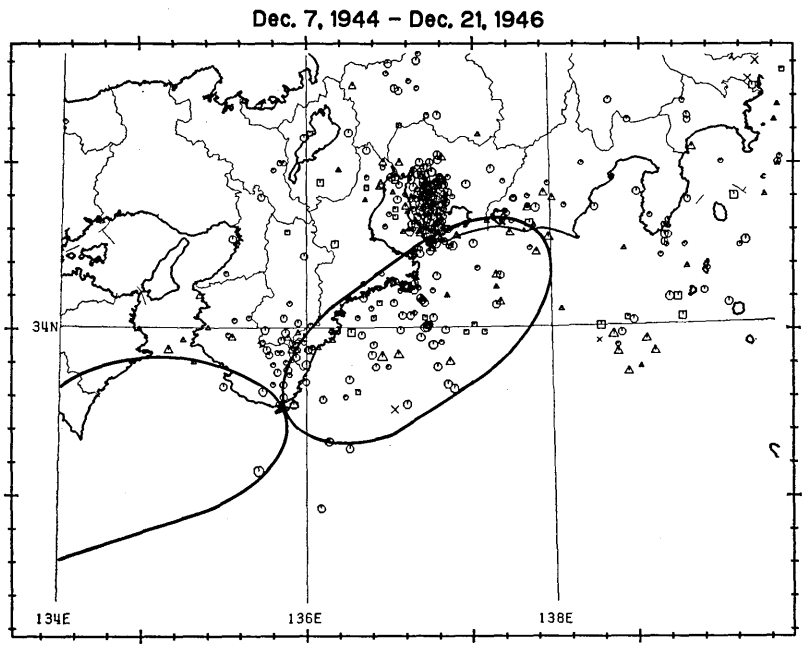

Fig. 35. The hypocenter distribution of earthquakes located by JMA for the period from the Tonankai earthquake to the Nankaido earthquake. Areas within the thick lines are the source regions of these great earthquakes. The dense distribution of hypocenters defines the source region of the Mikawa earthquake. For symbols, see the caption in Figure 5.

foreshock activity of the Mikawa earthquake in this case. There are the following three problems concerning the data. (1) In the list of felt earthquakes, earthquakes near land and habitation are sampled more than those offshore. (2) The list contains only vague information about hypocenters which is necessary to discriminate aftershocks from background activities or other activities unrelated to the main shock. (3) There must be the slowly decaying activity after the Tonankai earthquake which is as great as the Kanto earthquake studied before. The first helps to emphasize the foreshock activity of the Mikawa earthquake in the activity, since it occurred on land, while the greatest part of the source region for the Tonankai earthquake lies offshore. The second causes the inclusion of noises such as swarm activities in Wakayama Prefecture. The third might mask the quiescence. Those effects mar

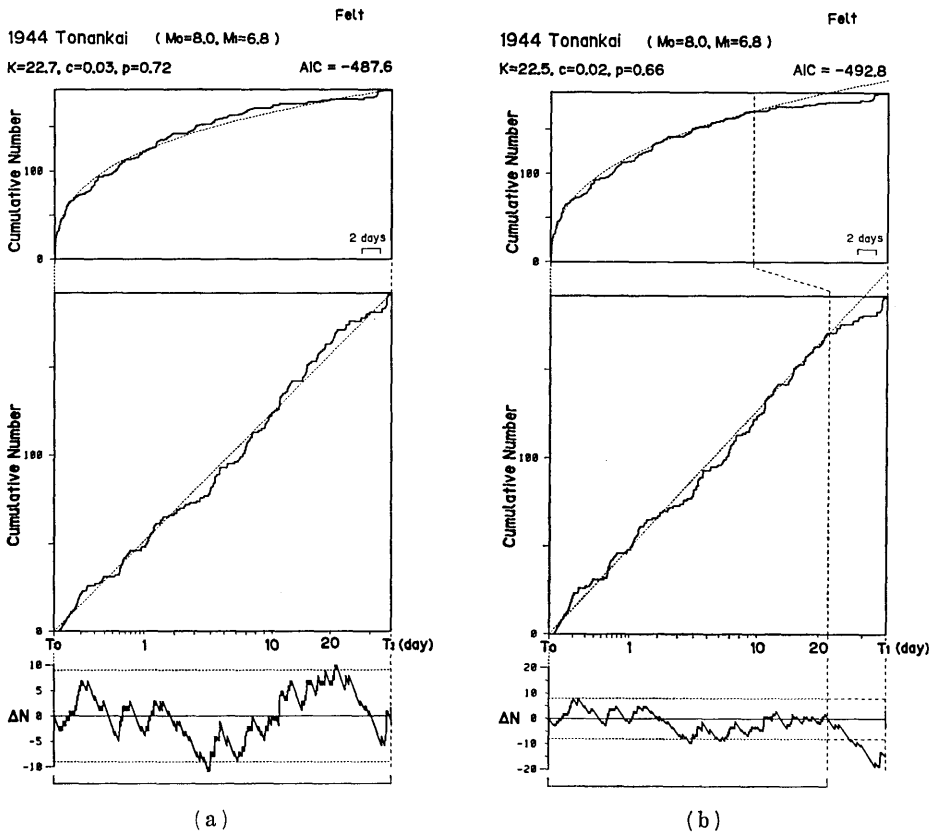

(a) (b)

Fig. 36. The aftershock sequence of the Tonankai earthquake during the period from the main shock to the Mikawa earthquake.
(a) FLT from all data.
(b) FLT for the first equation of (21).

the fit of the modified Omori formula throughout the normal stage of aftershock activity.

The number of felt aftershocks shows significant quiescence which is followed by active foreshocks of the Mikawa earthquake (Fig. 36(a)). The smallest AIC is for

$$n(t)=\begin{cases}\dfrac{22.5}{(t+0.02)^{0.66}} & T_0<t\leq Q_1\\ 0.9 & Q_1<t\leq R_1\\ 3.1 & R_1<t\leq T_1\end{cases} \tag{21}$$

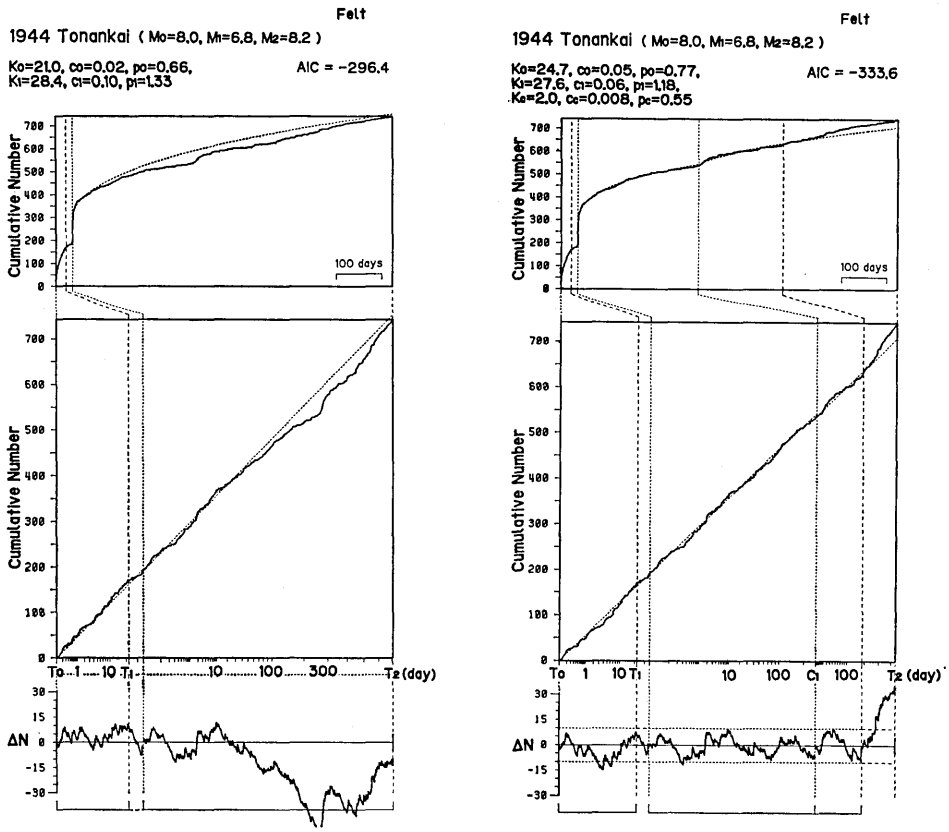

(a) (b)

Fig. 37. The aftershock sequence of the Tonankai earthquake until the time of the Nankaido earthquake.

(a) FLT for the model that the sequence is the combination of aftershock activities of the Tonankai and Mikawa earthquakes.

(b) FLT for the model including the induced activity by an M 6.0 deep earthquake at t=306 days and the further increase after t=490 days in addition to those considered in (a).

where $Q_1=22$ days and $R_1=33$ days (Fig. 36(b)). The first ten-day data still remain meandering around the expected line, although the degree of the deviation has decreased slightly.

A great earthquake in the eastern half of the Nankai trough usually occurs paired with one in the western half. The pair to the 1944 Tonankai earthquake is the Nankaido earthquake of M_S 8.2 (M_J 8.0) on December 21, 1946. Is there an activity change similar to the off Hachijo Island sequence between this pair of M 8 earthquakes?

The answer cannot be decided from the data of felt earthquakes (Fig. 37). The number of felt earthquakes in the Tonankai are increased after the occurrence of the M_J 6.0 deep earthquake off the Kii Peninsula on October 9, 1945 (Fig. 37(b)). The activity even increased eight months before the Nankaido earthquake. No quiescent stage is seen in the data.

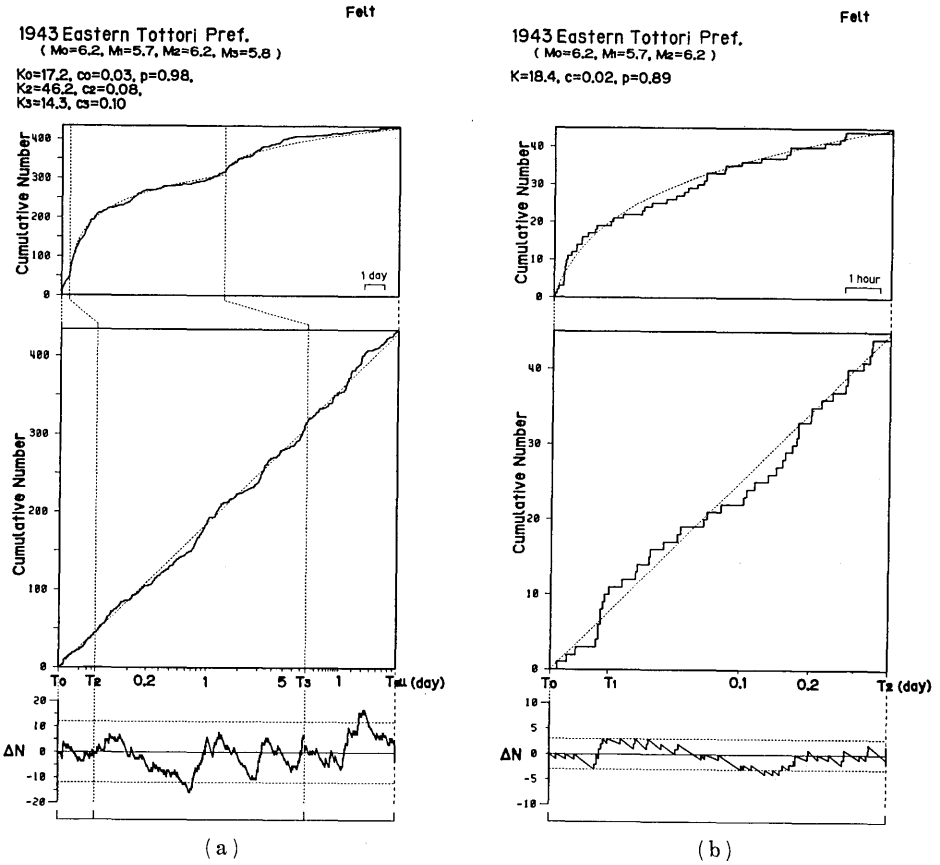

(a) (b)

Fig. 38. The sequence of the eastern Tottori Prefecture earthquake swarm.
(a) From the first M 6.2 earthquake to Mar. 31, 1943.
(b) From the first M 6.2 earthquake to the second M 6.2 earthquake.

The two-year period must be too long to expect the uniform observation of felt earthquakes, especially when the period contains frequent air raids and the end of the war. Small felt earthquakes are reported only with rough areas of occurrence and background activities are included in the data.

However, the quiescence in the aftershock activity of the Tonankai would not have existed before the Nankaido. If these two great earthquakes are paired by the effect through the asthenosphere, ordinary aftershocks of the first shock need not be sensitive to the preparatory process for the second one. Whether there was quiescence in this case is left unknown until suitable data will be discovered.

viii) The eastern Tottori Prefecture earthquake swarm of 1943

On March 4, 1943, an M_J 6.2 earthquake occurred in the eastern part of Tottori Prefecture. M_J 5.7, 6.2, and 5.8 earthquakes occurred after twenty minutes, ten hours, and eight days, respectively. This sequence is examined by the list of felt earthquakes in Geophysical Review of JMA.

The temporal characteristic of this sequence is not represented by the modified Omori formula (Fig. 38). The activity often increased without large earthquakes. The active stage alternated with the quiescent. The data meander largely around the straight line representing the fitted formula and estimated K-values are not proportional to magnitudes of main shocks as in other cases examined. The sequence of this type cannot be handled by the present analysis.

6. Discussion

i) Summary of results and other possible examples

In fourteen cases from nine sequences following the $M \geq 7$ main shocks, quiescence and recovered activity emerged in an aftershock activity before a large aftershock with secondary aftershock activity (Table 1, Figs. 39, 40). The anomalous change in activity (decrease then increase) prior to a large aftershock is larger than statistical fluctuations irrelevant to the large event. Only two among them are not statistically significant probably due to insufficient data.

Quiescence is not recognized in other four cases. Two aftershocks which triggered secondary aftershock activities in the 1984 western Nagano sequence are of M 5 and too small to affect the whole aftershock area of the main shock. The modified Omori formula is not applicable for the sequence before the Tanzawa earthquake of 1924. Definite results cannot be obtained for the sequence between the Tonankai and the Nankaido earthquakes from available data.

There are twenty-five other sequences in and around Japan between

Table 1. Sequences studied in this paper. Hypocenter coordinates are adopted from the catalog by Utsu (1982b). For the last two sequences, those from the Seismological Bulletin of JMA are adopted.

	i	[1]	T_i	Lat. (°N)	Long. (°E)	Depth (km)	M_S	M_J	M_{th}	K_i	c_i[2]	p_i[2]	Q_i	R_i-Q_i[3]	T_i-R_i[4]	R/Q t[5]	R/Q τ[6]
1	0		1923 Sept. 1 11:58	35.1	139.5	s[7]	8.2	7.9	5.4	5.2	0.07	1.62					
	1	a	2 11:56	34.9	140.2	s	7.7	7.3		0.1	0	0	0.2	0.25	0.55	2.2	0.7
	2	b	1924 Jan. 15 05:50	35.5	139.2	s		7.3					—	—	—	—	—
2	0		1943 Mar. 4 19:13	35.43	134.22	0		6.2	felt								
	1		19:35	35.47	134.17	10		5.7		17.2	0.03	0.98					
	2		5 04:50	35.50	134.22	0		6.2		46.2	0.08	*					
	3		13 00:24					5.8		14.3	0.10	*					
3	0		1944 Dec. 7 13:35	33.80	136.62	30	8.0	7.9	felt	24.7	0.05	0.77					
	1	c	1945 Jan. 13 03:38	34.68	137.07	0	6.8	6.8		27.6	0.06	1.18	22	11	3.6	0.3	0.2
	C_1		Oct. 9 19:56	33.82	136.93	340		6.0		2.0	0.008	0.55					
	2	d	1946 Dec. 21 04:19	33.03	135.62	20	8.2	8.0					—	—	—	—	—
4	0		1963 Oct. 12 20:26	44.70	149.18	20	7.0	6.3	4.5	9.2	0.49	1.27					
	1	e	13 14:17	44.89	149.56	0	8.1	8.1		73.4	*	*	(0.1)	(0.2)	(0.45)	(2.3)	(0.8)
	2	f	20 09:53	44.87	150.32	26	7.2	6.7		14.2	*	*	0.8[8]	4.7	0.8	0.2	0.1
	3	g	Nov. 16 06:06	44.28	149.16	0		6.2					16.3[8]	12.0	5.4	0.5	0.3
5	0		1964 June 16 13:01	38.35	139.18	40	7.5	7.5	4	54.0	0.31	1.29					
			13:17	38.80	139.03	0		6.1									
			15:53	38.63	139.20	0		6.1									
			16:14	38.37	139.32	20		6.1									
6	0		1968 May 16 09:48	40.73	143.58	0	8.1	7.9	≈3.7 4.5	190.4	0.21	1.13					
	1	h	19:39	41.42	142.85	40	7.7	7.5		32.2	0.43	0.91	(0.32)	(0.03)	(0.05)	(1.7)	(1.1)
	2	i	June 12 22:41	39.42	143.13	0	7.3	7.2		9.9	0.003	*	13	6.5	8	1.2	0.9

(To be continued)

Table 1. (Continued)

	i	1)	T_i	Lat. (°N)	Long. (°E)	Depth (km)	M_S	M_J	M_{th}	K_i	c_i 2)	p_i 2)	Q_i	R_i–Q_i 3)	T_i–R_i 4)	R/Q	
																t 5)	τ 6)
7	0		1972 Feb. 29 18:22	33.18	141.27	70	7.4	7.1	3.7	16.9	0.05	0.79					
	1	j	Dec. 4 19:16	33.20	141.08	50	7.5	7.2					165	70	44	0.6	0.5
8	0		1973 June 17 12:55	42.97	145.95	40	7.7	7.4	5.0	7.9	0.08	0.59					
	1	k	24 11:43	43.29	146.43	26	7.3	7.1		0.1	*	2.85	3	2	2	1	0.6
	2	l	27 07:31	43.01	146.66	10		6.5					8	1.3	0.5	0.4	0.3
9	0		1978 June 12 17:14	38.15	142.17	40	7.5	7.4	3.7	4.3	0.03	1.14					
	1	m	14 20:34	38.35	142.48	40		6.3		4.7	0.74	*	0.6	0.9	0.5	0.7	0.3
10	0		1983 May 26 12:00	40.36	139.08	14		7.7	4.0	46.0	0.19	1.23					
	C_1		June 1 08:19	40.77	139.30	27		5.1		6.0	*	*					
	1	n	9 21:49	40.22	138.90	23		6.1									
			22:03	40.19	138.86	14		6.0		2.6	*	*	11.2	2.3	0.9	0.4	0.3
	2	o	21 15:25	41.26	139.00	6		7.1					20.5	2	3.6	1.8	1.5
11	0		1984 Sept. 14 08:49	35.82	137.56	2		6.8	3.0	31.0	0.03	1.00					
	1	p	15 07:15	35.79	137.47	6		6.2		10.9	*	1.20	0.6	0.14	0.19	1.4	1.0
	2	q	Oct. 3 09:12	35.83	137.62	5		5.3		2.5	*	0.83	—	—	6	—	—
	3	r	1985 Feb. 26 19:54	35.84	137.58	8		5.0					—	—	5	—	—

1) The same symbols in Figure 40.
2) An asterisk shows that c_i or p_i is the same as c_{i-1} or p_{i-1}.
3) Duration of the quiescence.
4) Duration of the recovered activity.
5) Ratio of the duration of recovery to that of quiecence in the ordinary time unit.
6) The same ratio in the frequency-linearized time unit.
7) 's' in the depth column indicates shallow.
8) Time is measured from the mainshock (T_1) in this case.

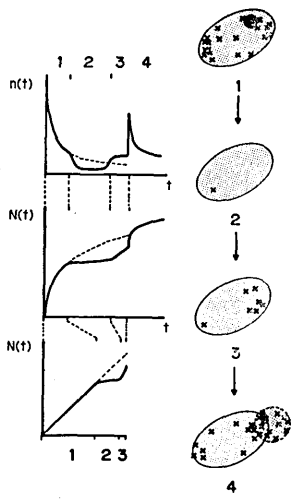

Fig. 39. A schematic illustration of the aftershock sequence including a large aftershock with precursory quiescence and recovery found in this study.
Stage 1. Ordinary aftershock activity.
Stage 2. Quiescence.
Stage 3. Recovered or foreshock activity.
Stage 4. Aftershock activity of the main shock and the secondary aftershock activity of the large aftershock.

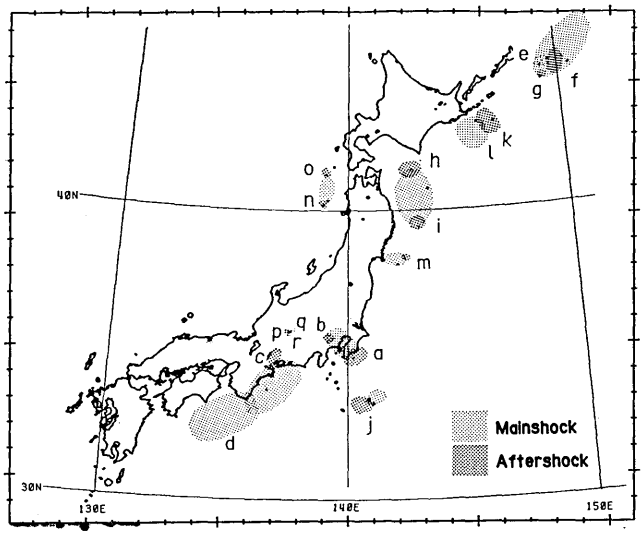

Fig. 40. Distribution of sequences studied in the present paper. Letters assigned for each aftershock correspond to those in the third column of Table 1.

Table 2. List of candidates for large shallow earthquakes accompanied by large aftershocks from 1926 to 1984 in and around Japan. Epicenter and magnitude of each event are adopted from the catalog byUtsu (1982b). Magnitude difference in parentheses is based on M_S. The second last column shows the approximate time interval between two earthquakes in minutes (m), hours (h), days (d), or months (M). 'S' and 'M' in the last column denote that the sequence is a swarm and a mixture of a swarm with an aftershock activity, respectively. 'D' in this column denotes that the data are not sufficient to draw any conclusion. Six sequences with 'A' in this column have the pattern of precursory changes.

	Date	Lat. (°N)	Long. (°E)	M_0	M_0-M_i	Delay	Type
1	1927 Mar. 7	35.53	135.15	7.3	0.8	1M	A
2	1928 May 27	39.95	143.25	7.0	0.3	1.3d	S
					0.5	5d	S
3	1931 Nov. 2	32.25	132.63	7.1	0.8	1h	D
4	1935 Sept. 11	42.90	146.33	7.4	0.5	21d	D
5	Oct. 18	40.75	144.35	7.1	0.6	15h	S
6	1936 Nov. 3	38.15	142.13	7.5	0.9	2M	A
					0.4	9M	A
7	1937 Feb. 21	44.5	149.5	7.6	0.9	1.5d	D
8	1938 May 23	36.65	141.58	7.0	0.5	4M	M
					1.0	5M	M
9	Nov. 5	37.33	142.18	7.5	0.2	2h	S
					0.1	1d	S
10	1939 Oct. 11	38.28	142.78	7.0	0.6	19m	D
11	1941 Nov. 19	32.02	132.08	7.2	0.9	9M	M
12	1943 June 13	41.25	143.35	7.1	0.4	2d	D
13	Sept. 10	35.52	134.08	7.2	1.0	1d	D
14	1945 Feb. 10	41.00	142.07	7.1	0.9	8d	A
15	1946 Dec. 21	33.03	135.62	8.0	1.0	16M	D
16		44.1	148.2	7.2	1.0	10h	D
					0.9	10h	D
					0.7	13d	D
17	1953 Nov. 26	33.98	141.72	7.4	0.8	15h	D
18	1958 Nov. 7	44.38	148.58	8.1	1.2	6d	D
					(0.9)		
19	1960 Mar. 21	39.83	143.43	7.2	0.5	2d	M
20	1961 Feb. 27	31.60	131.85	7.0	1.0	9M	M
21	Aug. 12	42.85	145.57	7.2	0.3	3M	A
22	1968 Apr. 1	32.28	132.53	7.5	1.2	6.5h	D
23	1975 June 10	43.18	147.36	7.0	0.5	3d	A
24	1978 Jan. 14	34.77	139.25	7.0	1.2	1d	A
25	Mar. 23	44.70	148.17	7.0	−0.3	1.5d	D

1926 and 1984 whose main shock magnitude M_0 is 7.0 or over and were followed by aftershocks of magnitude M_0-1.2 or more (Table 2). The temporal characteristics cannot be represented by the modified Omori formula in seven cases of them. The number of aftershocks in JMA catalogs is too small due to the short time interval between the main shock and the large aftershock or the limit of ability of the JMA network in twelve cases. In the remaining six cases, there seems to be a pair of the quiescent and recovered stages before a large aftershock. However, the quality of JMA data is low for statistical analysis.

One of them, the sequence after the off Izu-Oshima Island earthquake of 1978 (No. 24 in Table 2), was studied by TSUMURA *et al.* (1978) with microearthquake observation. Although the drum-recording system in the local network at that time impeded making a homogeneous list of aftershocks before the largest aftershock at Nekkoh pass near the western end of the main fault, there was a similar pattern of quiescence and recovery of activity mostly in the western part of the fault zone prior to the largest aftershock as seen in their Figure 19.

A similar pattern is also recognized in sequences occurring outside of Japan. In the Chile sequence of 1960, there were also the quiescent and recovered periods in the aftershock activity of the M_S 7.9 initial shock before the great Chile earthquake of M_S 8.5, as shown in Figure 5 of LOMNITZ and HAX (1966). Changes in aftershock activity before a large aftershock have been reported for six sequences in China (WANG and WANG, 1983). Main shocks were of M 6.8~7.9 which were followed by aftershocks of M 5.2~7.2 with secondary aftershock activities. According to them, the deviation of the aftershock occurrence rate became large and the rate increased before a large aftershock. Since they used the daily frequencies of aftershocks even for scores of days after the main shock, largely deviated parts in their plots correspond to low occurrence-rate periods, some of which may be the quiescence prior to large aftershocks. Although the one-day period following the main shock was excluded from all plots and a time axis was a mere logarithmic scale of lapse time from the main shock even after an apparent secondary aftershock activity was added, quiescence and increase of activity were seen before a large aftershock in some of their examples.

All these cases cannot be analyzed in the same manner as that of this study. However, similar patterns seen in the other cases in Japan and the other areas of the world ensure that the emergence of quiescence and recovery in aftershock activity of the main shock prior to a large aftershock is universal.

ii) Application to earthquake prediction

Can this precursory change in aftershock activity be used for real-time prediction of a large aftershock? When aftershock activity is checked regularly with AIC in real time, quiescence can be detected by the time a large aftershock occurs. However, it is preferable that quiescence is detected well in advance. In a case like the change before the largest aftershock of the off Iturup Island earthquake of 1963, it is easy. When a curve for cumulative number of aftershocks is drawn against an ordinary time axis in real time, the quiescence is easily found on the plot soon after it starts in this case (Fig. 33). The anomaly in the aftershock activity of the Kanto earthquake of 1923 before the off Katsuura earthquake is also found easily (Fig. 11). However, calculation of the parameters is required for finding the starting point of quiescence Q in most cases.

The change of parameter values in the modified Omori formula, especially the anomalous change of p-value, is one element for detection. The p-value becomes gradually higher after Q in the case of the western Nagano Prefecture earthquake of 1984, which is mentioned in 4-ii). However, in the case of the east off Hachijo Island earthquake of 1972, the p-value varies within a normal range even after Q (Fig. 41). Therefore, real-time pursuit of only the parameter values is not a reliable method for detecting the quiescence.

Checking the b-value is also not promising for the early detection of quiescence. An increase in b-value during the quiescence is recognized. However, the b-value cannot be determined precisely without a lot of data and it is not a good parameter to detect a seismicity anomaly in the early stage.

In analyzing the whole period of a sequence, a plot of a cumulative number against the frequency-linearized time is efficient to find the activity change. When the whole sequence is shown on a plot with the frequency-linearized time that is estimated from data until Q, the quiescent and recovered stages are distinct on the plot (Fig. 1 (b)). If the cumulative number of aftershocks is checked regularly in real time on the plot against the frequency-linearized time revised at each check, we have a good chance at detecting quiescence soon after it begins. If Q is detected, the frequency-linearized time should be fixed and the further sequence is plotted against it. On this plot, R can be detected as the point where the gradient of the observed cumulative number curve starts to re-increase.

Suppose K^T, c^T and p^T are the maximum likelihood estimates for data until T.

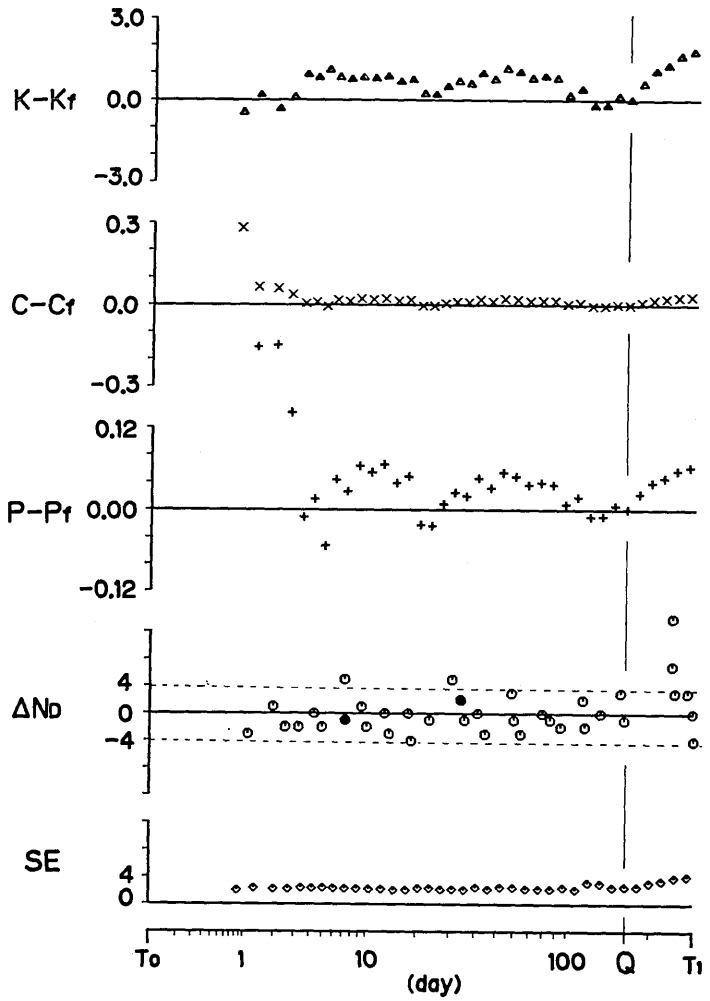

Fig. 41. An example of the real-time watch of an aftershock activity. The case of the east off Hachijo Island earthquake is shown. K^T, c^T, and p^T (see (22) for the definition) for various T are shown in the upper three graphs as differences from values for the final model of (8-1). Time axis for all graphs is shown at the bottom, which is proportional to the frequency-linearized time defined by (8-1). Note that when $T \geq 3$ days (that is, when the cumulative number of aftershocks used for the estimation of parameters are more than 60), K^T, c^T, and p^T are not largely different from the final values and not dependent on T. The standard error of data, σ^T (see (30)) is also shown in the bottom graph. ΔN_D (see Figure 42 and (28)) for each T is shown (for the case of $n=5$) in the fourth graph from the top at the time of t_R for each T. Broken line in the graph show $2\sigma^T|_{T=Q}$ for the reference. The first ΔN_D is calculated for $T=0.85$ day. The next ΔN_D is calculated for $T=t_p{}^T|_{T=0.85}=1.2$ day. Then the next ΔN_D is for $T=t_p{}^T|_{T=1.2}=2.0$ day, the next is for $T=t_p{}^T|_{T=2.0}$, and so forth. For solid circles in this graph, see the text.

$$\ln L\,(K^T, c^T, p^T) = \max.\ln L\,(K, c, p\,; t_i \leq T) \tag{22}$$

The observed cumulative number of aftershocks until T is reprensented as $N(T)$. The frequency-linearized time τ^T is equivalent to the predicted cumulative number of aftershocks $N_p{}^T(t)$ until t.

$$\tau^T(t) = \int_0^t \frac{K^T}{(s+c^T)^{p^T}} ds = N_p{}^T(t) \tag{23}$$

When the sequence is plotted against this frequency-linearized time,

$$\Delta N(t) = N(t) - N_p{}^T(t) \tag{24}$$

indicates the difference of the actual cumulative number of aftershocks at time t from the estimated one with data until T. Suppose X^T is the inverse function of τ^T.

$$t = X^T(N_p{}^T) \tag{25}$$

$$t_p{}^T = X^T(N(T)+n) \tag{26}$$

The time $t_p{}^T$ defined by (26) is the predicted time for the occurrence of n afterhocks. It is predicted that n aftershocks occur by $t_p{}^T$, while they actually occur by t_R (Fig. 42).

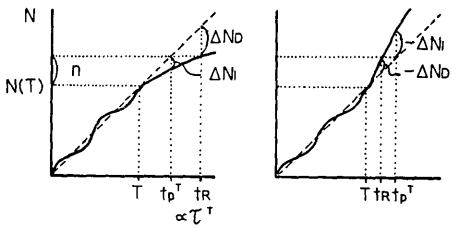

Fig. 42. Schematic graph explaining ΔN_D and ΔN_I. The cumulative number is shown against τ^T.

$$N(t_R) = N(T) + n \tag{27}$$

When t is taken as t_R or $t_p{}^T$,

$$\Delta N_D = -\Delta N(t_R) = N_p{}^T(t_R) - (N(T)+n) \geq -n \tag{28}$$

or

$$\Delta N_I = -\Delta N(t_p{}^T) = (N(T)+n) - N(t_p{}^T) \leq n \tag{29}$$

indicates the consistency of the data after T with those until T. When the activity decreases largely after T, ΔN_D becomes a large positive

number. When the activity increases largely after T, ΔN_I becomes a large negative number (Fig. 42). In order to find Q, ΔN_D is useful.

Since the data even without any significant anomaly show some sampling fluctuations around the fitted modified Omori formula, we need a threshold to discriminate anomalous ΔN_D from mere fluctuation. When the threshold is determined, n is determined as some number larger than the threshold but not too large in order to detect Q early. The standard deviation of ΔN_D is related to T, n, errors in estimation of K^T, c^T, and p^T, and the standard deviation σ^T of data until T

$$\sigma^T = \sqrt{\frac{\sum_{t_i \leq T} \{N(t_i) - N_p{}^T(t_i)\}^2}{N(T)}}, \tag{30}$$

in a complicated way. In the bottom graph of Figure 3 (b) or similar figures, $\Delta N(t)$ is plotted against τ^T where $T=Q$, and $2\sigma^T$ is also shown by dotted lines. $|\Delta N(t)|$ is usually smaller than $2\sigma^T$ when $t<T=Q$ in those graphs. Therefore, $2\sigma^T$ may be effective to distinguish abnormal value of ΔN_D from normal ones, since ΔN_D is $-\Delta N(t)$ for $t>T$. Whether $2\sigma^T$ is effective or not is examined for the homogeneous data of the off Hacnijo Island sequence (Fig. 41).

For this example, the threshold of $2\sigma^T$ is successful. However, the beginning of the quiescence should be announced when ΔN_D exceeds this threshold in consective checks. For $T<Q$, σ^T is about 2. In Figure 41, ΔN_D for $n=5$ is shown. ΔN_D is usually smaller than 4 when $t_R<Q$. However, ΔN_D sometimes exceeds this threshold even $t_R<Q$. In the next check (shown by a solid circle in Figure 41) with the frequency-linearized time revised by data until $t_p{}^T$, ΔN_D returns to be smaller than 4 for such a case. When the quiescence begins, ΔN_D stays larger than the threshold. When T increases further, σ^T increases and ΔN_D decreases, since τ^T is obtained from data including the anomaly. When n is between 5 and 8, the beginning of the quiescence can be recognized by ΔN_D as it exceeds the threshold of 4 in consecutive checks.

To what extent can we predict a large aftershock? If quiescence and recovery are observed in the real time check of an aftershock activity following a large shallow earthquake, an aftershock as large as the main shock is expected soon. The rough location of this large aftershock is also estimated from checking hypocenters of aftershocks during the recovered stage. However, the precise magnitude and time of occurrence of the large aftershock cannot be predicted. In fourteen examples investigated in this paper, there seems to be no such a useful relation for predicting the size or the time as suggested in other earthquake prediction studies (e. g. SCHOLZ *et al.*, 1973; OHTAKE, 1980; MOTOYA, 1984)

(Table 1). The actual time interval from the main shock to the large aftershock varies from ten hours to nine months. The length of the quiescent and recovered stages also varies from one hour to several tens of days. The ratio of the length of the recovered stage to that of the quiescence varies from 0.1 to 1.5 even on the frequency-linearized time unit.

iii) A model for the cause of large aftershocks

There is no established theory for the occurrence of aftershocks. Advocated theories can be classified into two groups. One is that an aftershock is the re-fracture of a part of the fault ruptured during the main shock. The other is that an aftershock is the fracture in a part which remained unruptured during the main shock.

The former type requires some mechanisms for recovery of stress on some parts of the fault relieved by the main shock, and sticking the surface of the fault to restore stress again. Models of this type use the property of time-dependent friction with some viscoelastic process (DIETERICH, 1972) such as consolidation (BOOKER, 1974). However, these models have some defects. For the viscoelasticity of standard linear solid, a relaxation time of a few days is required for a realistic simulation of an aftershock activity. This relaxation time seems to be too short for the crustal rocks. If consolidation is the process of reloading stress on the fault, some migration or expansion of an aftershock activity within the source region of the main shock may be observed with a flow of pore fluid. However, aftershocks were observed in the entire source region immediately after the main shock (e. g. PAGE, 1968; MATSU'URA, 1983). Time-dependent friction is rather a good explanation for the sticking process of a fault for the next main shock.

Models of the latter type are based on the decrease of strength in some remaining parts due to a pore fluid flow (NUR and BOOKER, 1972), or stress corrosion (SCHOLZ, 1968, 1972; ANDERSON and GREW, 1977; DAS and SCHOLZ, 1981; OHNAKA, 1983). If a change of pore pressure is the cause of decreased strength, water or some liquid is necessary, while stress corrosion only requires H_2O vapor or some corrosive gas. Stress concentration at edges around remaining parts may have as important role in starting the rupture in those parts after they are weakened (KNOPOFF, 1972). Models of this type agree well with the observation that many aftershocks occur near edges of the fault of the main shock.

The cause of the emergence of quiescence before the main shock is also not established yet. When the dilatancy model (e. g. SCHOLZ *et al.*, 1973) dominated the world in the early 1970's, dilatancy hardening was considered as the complete explanation for quiescence. However, it be-

came obsolete after the V_p/V_s anomaly and other anomalies on which the dilatancy model was based were suspected as fallacious (e. g. EVERNDEN, 1982).

Recently, models were proposed explaining seismic patterns prior to the main shock or of the entire seismic cycle by heterogenity of faults (MOGI, 1977; TSUMURA, 1979; KANAMORI, 1981; MIKUMO and MIYATAKE, 1983). According to these models, quiescence appears when parts with certain strengths do not exist in a fault. Therefore, the emergence of quiescence is destined by the material property of a fault and not always required before the main shock.

The model proposed by OHNAKA (1984) includes delayed fracture in precursory seismicity. While stress is accumulating on a locked fault, precursory activity is induced. When the premonitory slip starts on the fault, stress is held constant. Under this constant stress, stress corrosion causes decaying precursory activity. Quiescence emerges after precursory activity decays completely and before the stress instability occurs, the final stage in generating the main shock. If the final stage comes before the precursory activity decays completely, there is no quiescence between precursory activity and foreshocks.

It is very difficult to construct a perfect model explaining the precursory pattern found in this study, since little is known about physical processes of an earthquake or an aftershock. Furthermore, a model explaining the preseismic process together with the occurrence of aftershock is not yet proposed. The quiescence before the main shock may emerge through a process different from that of the quiescence before a large aftershock. The generating process of a large aftershock may start after the main shock and the duration of the process may be much shorter than that of the main shock. However, recent models of the quiescence before the main shock suggest that heterogeneity of the area may affect the temporal pattern of seismicity greatly.

A model should agree with the following features found in this study. Before a small aftershock which is followed by secondary aftershocks, quiescence is not seen in the aftershock activity in the entire source region of the main shock. The recovered activity is very high in some cases and apparently constitutes the foreshock activity of the coming large aftershock. It is just the level expected from the modified Omori formula fitted before the quiescence begins in some cases. The length of the anomalous pattern ranges from an hour to months. In other words, the rapidity of the process for generating a large aftershock varies from place to place or from case to case.

A possible model explaining the anomalous pattern before a large aftershock found in this paper can be made with the heterogeneity of

porosity in the source region. Suppose that aftershocks are delayed fractures of remaining parts and some of those are formed of rocks with porosity quite lower than others. The ordinary aftershock activity continues while fracture of parts of ordinary porosity covers the redistribution of stress in the source region. However, stress redistribution is obstructed after a certain period, since fracture of low porosity parts is delayed more than the other parts. It takes longer to weaken low porosity rocks, since the soaking velocity of corrosive vapor or pore fluid into rocks depends on porosity. Therefore, the aftershock activity in the entire source region decreases from the normal level expected in the modified Omori formula, until the low porosity parts are sufficiently weakened. Then shocks mostly occur around these parts, since stress is concentrated around them. Final fracture of a large low porosity part triggers the fracture of the adjacent region. After this large aftershock, secondary aftershocks occur. Aftershocks in the main shock source region also occur after the large aftershock, since stress redistribution in the source region resumes.

This model provides one possibility. In order to explain the generating process of a large aftershock and the cause of the quiescence prior to it, various kinds of data other than the activity anomaly studied in this paper are necessary. Experimental studies of stress corrosion or behavior of pore fluid are also important for solving this problem. The theoretical approach to the dynamic stress redistribution among cracks may give some constraints to the model. Further research on the process from various fields is necessary.

7. Conclusion

An anomalous pattern has been found in aftershock activities prior to large aftershocks which are followed by secondary aftershocks and are not smaller than the main shock by more than 1.2 unit of magnitude. Before the occurrence of such a large aftershock, the whole aftershock area of the main shock becomes quiescent. In the quiescent stage, the frequency of larger aftershocks decreases more; in other words, the *b*-value increases. Then the aftershock activity recovers to the normal level or increases beyond the normal level prior to the large aftershock. This recovered activity tends to cluster near the hypocenter of the forthcoming large afershock. This pattern is not recognized in aftershock activities not accompanied by large aftershocks.

Based on this feature, prediction of a large aftershock is possible when a real-time check of the aftershock activity change is continued with due care for the homogeneity of the data. However, an accurate

preannouncement of the size and occurrence time is impossible by this method, because there is no nice relation indicating the size or the time of the coming large aftershock. We can only expect that an aftershock which may be as large as the main shock will occur after the recovered period of one-fifth to twice as long as the quiescent period near the place where most shocks occur during the recovery period.

The mechanism of the emergence of the precursory pattern before a large aftershock is a difficult but interesting problem. A model assuming low porosity parts in the source region of the main shock can explain features found in this study. However, a more complete answer should be sought in future studies with various approaches to this problem.

Acknowledgments

I am very grateful to Prof. Tokuji Utsu for his helpful suggestions, continuous encouragment throughout this work, and critical reading of the manuscript. Discussions with Dr. Yosihiko Ogata, Profs. Mitiyasu Ohnaka, Kunihiko Shimazaki, Katsuyuki Abe, and Ryosuke Sato were helpful. I thank Mr. Ikuo Karakama very much for all his help in my struggle with old original records and routine data. Dr. Kenshiro Tsumura gave me valuable advice concerning the old data of both the Earthquake Research Institute (ERI) and JMA, and access to the old routine data of ERI. The former and the present staff of the Dodaira Microearthquake Observatory and commissioned persons who operated untelemetered stations contributed greatly in gathering the valuable microearthquake observational data in the Kanto District without which this study could not have been started. Profs. Harumi Aoki and Takeshi Mikumo kindly gave me valuable information about the western Nagano Prefecture earthqukae. Mr. Yuzo Ishikawa helped me in searching papers written in Chinese. Dr. Kathy Jackson kindly read the manuscript and improved my English. For calculating the maximum likelihood solution for parameters of the modified Omori formula, subroutines written by Dr. Y. Ogata at the Institute of Statistical Mathematics were used. Computations and data processing were done with a HARRIS H-300 at the Seismological Mobile Survey of the Earthquake Research Institute, the University of Tokyo.

References

ABE, K., 1981, Magnitudes of large shallow earthquakes from 1904 to 1980, *Phys. Earth Planet. Interiors*, **27**, 72-92.

AKAIKE, H., 1974, A new look at the statistical model identification, *IEEE Trans. Autom. Control* **AC-19**, 716-723.

AKI, K., 1965, Maximum likelihood estimate of b in the formula $\log N=a-bM$ and its confidence limits, *Bull. Earthq. Res. Inst., Univ. Tokyo*, **43**, 237-239.

ANDERSON, O. L. and P. C. GREW, 1977, Stress corrosion theory of crack propagation with applications to geophysics, *Rev. Geophys. Space Phys.*, **15**, 77-104.

BOOKER, J. R., 1974, Time dependent strain following faulting of a porous medium, *J. Geophys. Res.*, **79**, 2037-2044.

DAS, S. and C. H. SCHOLZ, 1981, Theory of time-dependent rupture in the earth, *J. Geophys. Res.*, **86**, 6039-6051.

DIETERICH, J. H., 1972, Time-dependent friction as a possible mechanism for aftershocks, *J. Geophys. Res.*, **77**, 3771-3781.

EVERNDEN, J. F., 1982, Earthquake prediction: what we have learned and what we should do now, *Bull. Seismol. Soc. Am.*, **72**, S343-S349.

HORI, M., 1973, Determination of earthquake magnitude of the local and near earthquake by the Dodaira microearthquake observatory, *Spec. Bull. Earthq. Res. Inst., Univ. Tokyo*, **10**(4), 1-4 (in Japanese).

INOUYE, W., 1965, On the seismicity in the epicentral region and its neighbourhood before the Niigata earthquake, *Quart. J. Seismol.*, **29**, 139-144 (in Japanese).

ISHIDA, M. and H. KANAMORI, 1978, The foreshock activity of the 1971 San Fernando earthquake, California, *Bull. Seismol. Soc. Am.*, **68**, 1265-1279.

JMA, 1965, The report on the Niigata earthquake, 1964, *Technical Rep. JMA*, **43**, ch 1, 5-27 (in Japanese).

JMA, 1969, The report on the Tokachi-oki earthquake, 1968, *Technical Rep. JMA*, **68**, ch 1, 6-20 (in Japanese).

JMA, 1974, The report on the Nemuro-hanto-oki earthquake of June 17, 1973, *Technical Rep. JMA*, **87**, ch 1, 4-13 (in Japanese).

KANAMORI, H., 1981, The nature of seismicity patterns before large earthquakes, in *Earthquake Prediction—an international review*, Maurice Ewing Series 4, edited by D. W. Simpson and P. G. Richards, pp. 1-19, American Geophysical Union, Washington D. C.

KNOPOFF, L., 1972, Model for aftershock occurrence, in *Flow and Fracture of Rocks*, Geophysical Monograph 16, edited by H. C. Heard, I. Y. Borg, N. L. Carter, and C. B. Raleigh, pp. 259-263, American Geophysical Union, Washington D. C.

LOMNITZ, C. and A. HAX, 1966, Clustering in aftershock sequences, in *the Earth beneath the Continents*, Geophysical Monograph 10, edited by J. S. Steinhart and T. J. Smith, pp. 502-508, American Geophysical Union, Washington D. C.

MATSU'URA, M., 1984, Bayesian estimation of hypocenters with origin time eliminated, *J. Phys. Earth*, **32**, 469-483.

MATSU'URA, M., T. TANIMOTO and T. IWASAKI, 1981, Quasi-static displacements due to faulting in a layered half-space with an intervenient viscoelastic layer, *J. Phys. Earth*, **29**, 23-54.

MATSU'URA, R. S., 1983, Detailed study of the earthquake sequence in 1980 off the east coast of the Izu Peninsula, Japan, *J. Phys. Earth*, **31**, 65-101.

MIKUMO, T. and T. MIYATAKE, 1983, Numerical modelling of space and time variations of seismic activity before major earthquakes, *Geophys. J. R. astr. Soc.*, **74**, 559-583.

MIZOUE, M., M. NAKAMURA, N. SETO, K. SAKAI, M. KOBAYASHI, T. HANEDA and S. HASHIMOTO, 1985, A concealed fault system as inferred from the aftershock activity accompanying the 1984 western Nagano Prefecture earthquake of M 6.8, *Bull. Earthq. Res. Inst., Univ. Tokyo*, **60**, 199-220 (in Japanese).

MOGI, K., 1962, On the time distribution of aftershocks accompanying the recent major earthquakes in and near Japan, *Bull. Earthq. Res. Inst., Univ. Tokyo*, **40**, 107-124.

MOGI, K., 1968a, Development of aftershock areas of great earthquakes, *Bull. Earthq. Res. Inst., Univ. Tokyo*, **46**, 175-203.

MOGI, K., 1968b, Some features of recent seismic activity in and near Japan (1), *Bull.*

Earthq. Res. Inst., Univ. Tokyo, **46**, 1225-1236.

MOGI, K., 1969, Some features of recent seismic activity in and near Japan (2), *Bull. Earthq. Res. Inst., Univ. Tokyo*, **47**, 395-417.

MOGI, K., 1977, Seismic activity and earthquake prediction, in *Proc. Symp. Earthq. Pred. Res.*, pp. 203-214, Seismological Society of Japan (in Japanese).

MOTOYA, Y., 1984, Study of seismicity in and around Hokkaido with relation to earthquake prediction, D. Sc. thesis, Hokkaido Univ., pp. 124 (in Japanese).

MOTOYA, Y. and K. ABE, 1985, Waveform similarity among foreshocks and aftershocks of the October 18, 1981, Eniwa, Hokkaido, earthquake, *Earthq. Pred. Res.*, **3**, 627-636.

NUR, A. and J. R. BOOKER, 1972, Aftershocks caused by pore fluid flow? *Science*, **175**, 885-887.

OGATA, Y., 1983, Estimation of the parameters in the modified Omori formula for aftershock frequencies by the maximum likelihood procedure, *J. Phys. Earth*, **31**, 115-124.

OGATA, Y. and K. SHIMAZAKI, 1984, Transition from aftershock to normal activity: the 1965 Rat Islands earthquake aftershock sequence, *Bull. Seismol. Soc. Am.*, **74**, 1757-1765.

OGATA, Y. and K. KATSURA, 1986, Point process model with linearly parameterized intensity for the application to earthquake data, in *Essays in Time Series and Allied Processes*, edited by J. Gani and M. B. Priestly, pp. 291-310, Applied probability trust.

OHNAKA, M., 1983, Acoustic emission during creep of brittle rock, *Int. J. Rock Mech. Min. Sci. Geomech. Abstr.*, **20**, 121-134.

OHNAKA, M., 1984, A sequence of seismic activity in the Kanto area precursory to the 1923 Kanto earthquake, *Pageoph*, **122**, 848-862.

OHTAKE, M., 1980, Earthquake prediction based on the seismic gap with special reference to the 1978 Oaxaca, Mexico earthquake, *Rep. National Res. Center Disaster Prevention*, **23**, 65-110 (in Japanese).

OHTAKE, M., T. MATSUMOTO and G. LATHAM, 1977, Seismicity gap near Oaxaca, southern Mexico as a probable precursor to a large earthquake, *Pageoph*, **115**, 375-385.

PAGE, R., 1968, Aftershocks and microaftershocks of the great Alaska earthquake of 1964, *Bull. Seismol. Soc. Am.*, **58**, 1131-1168.

THE PARTY FOR AFTERSHOCK OBSERVATION, 1968, Observation of aftershocks of the Niigata earthquake of June 16, 1964, *Bull. Earthq. Res. Inst., Univ. Tokyo*, **46**, 205-221.

SANTO, T., 1964, Shock sequences of the southern Kurile Island from October 09 to December 31, 1963, *Bull. Internat. Inst. Seismol. Earthq. Engineer.*, **1**, 33-54.

SCHOLZ, C. H., 1968, Microfractures, aftershocks and seismicity, *Bull. Seismol. Soc. Am.*, **58**, 1117-1130.

SCHOLZ, C. H., 1972, Static fatigue of quartz, *J. Geophys. Res.*, **77**, 2104-2114.

SCHOLZ, C. H., L. R. SYKES and Y. P. AGGARWAL, 1973, Earthquake prediction: a physical basis, *Science*, **181**, 803-810.

SCHOOL OF SCIENCE, NAGOYA UNIVERSITY, 1985, The western Nagano Pref. earthquake, 1984, *Rep. Coord. Comm. Earthq. Pred.*, **33**, 123-134 (in Japanese).

TSUJIURA, M., 1979, The difference between foreshocks and earthquake swarms, as inferred from the similarity of seismic waveform (Preliminary report), *Bull. Earthq. Res. Inst., Univ. Tokyo*, **54**, 309-315 (in Japanese).

TSUMURA, K., 1967, Determination of earthquake magnitude from total duration of oscillation, *Bull. Earthq. Res. Inst., Univ. Tokyo*, **45**, 7-18.

TSUMURA, K., 1979, A model for temporal variation of seismic activity and precursors, *Abstr. Seismol. Soc. Japan*, **No. 1**, p. 159 (in Japanese).

TSUMURA, K., I. KARAKAMA, I. OGINO and M. TAKAHASHI, 1978, Seismic activities before and after the Izu-Oshima-kinkai earthquake of 1978, *Bull. Earthq. Res. Inst., Univ. Tokyo*, **53**, 675-706 (in Japanese).

UTSU, T., 1961, A statistical study on the occurrence of aftershocks, *Geophys. Mag.*, **30**, 521-605.

UTSU, T., 1965, A method for determining the value of b in a formula $\log n = a - bM$ showing the magnitude-frequency relation for earthquakes, *Geophys. Bull. Hokkaido Univ.*, **13**, 99-103 (in Japanese).

UTSU, T., 1968, Seismic activity in Hokkaido and its vicinity, *Geophys. Bull. Hokkaido Univ.*, **20**, 51-75 (in Japanese).

UTSU, T., 1969, Aftershocks and earthquake statistics (I)—some parameters which characterize an aftershock sequence and their interrelations, *J. Faculty Sci. Hokkaido Univ., Ser. VII*, **3**, 129-195.

UTSU, T., 1970, Seismic activity and seismic observation in Hokkaido in recent years, *Rep. Coord. Comm. Earthq. Pred.*, **2**, 1-2 (in Japanese).

UTSU, T., 1979, Seismicity of Japan from 1885 through 1925—a new catalog of earthquakes of $M \geq 6$ felt in Japan and smaller earthquakes which caused damage in Japan, *Bull. Earthq. Res. Inst., Univ. Tokyo*, **54**, 253-308 (in Japanese).

UTSU, T., 1981, Seismicity of central Japan from 1904 through 1925, *Bull. Earthq. Res. Inst., Univ. Tokyo*, **56**, 111-137 (in Japanese).

UTSU, T., 1982a, Seismicity of Japan from 1885 through 1925 (Corrections and supplement), *Bull. Earthq. Res. Inst., Univ. Tokyo*, **57**, 111-117 (in Japanese).

UTSU, T., 1982b, Catalog of large earthquakes in the region of Japan from 1885 through 1980, *Bull. Earthq. Res. Inst., Univ. Tokyo*, **57**, 401-463 (in Japanese).

UTSU, T., 1982c, Relationships between earthquake magnitude scales, *Bull. Earthq. Res. Inst., Univ. Tokyo*, **57**, 465-497 (in Japanese).

WANG, B. and C. WANG, 1983, Temporal and spatial features of aftershock sequences, *Acta Seismologica Sinica*, **5**, 383-396 (in Chinese).

大きい余震の発生前の本震の余震活動度の異常

地震研究所　松　浦　律　子

地震活動から大きい地震の発生のメカニズムを解明し，地震予知に役立てる為には，大きい地震の準備段階を反映した地震活動度が，通常の状態におけるものとどの様にどの程度異なっているかを，定量的に把握することが必要である．そこで現在最もよく通常の時系列的性質を定量的に取り扱える余震活動に着目し，大きい地震の発生前に何らかの特徴的な活動度の変化が生じるかどうかを検討した．即ち，二次余震を伴う様な大きい余震の発生前に，本震の余震活動が通常の改良大森公式から変化するか否か，日本附近で解析可能なデータのある例，9 活動中の 18 例について調査した．

この結果，大きい余震の発生前には，一旦本震の余震域全体の余震活動度が改良大森公式から予測されるレベルの数分の一以下に低下する静穏期が出現し，これが再び予測されるレベルに回復或いはより活発化して大きい余震が発生するという変化が広く認められることを見出した．さらに，静穏期には b 値が増加し大きめの余震程発生し難くなっていること，回復後の活動は主として将来発生する大きい余震の震源附近に分布することを見出した．この様な余震活動度の変化は，大きい余震の発生と無関係な単なる活動度のゆらぎより数倍大きい．

この性質を利用して，本震直後から慎重な余震活動の監視を行なうことによって，新たな被害をもたらす様な大きい余震の発生を予報できることが期待されるが，静穏期・回復期の期間長，両者の比，発生する余震の規模等の間に詳細な発生時刻や規模の予知に役立つ様な明瞭な規則性はみられなかった．
